

WEC Development Project

Winter Semester 2025/2026

Final Design Report



OPTIMUS
SYRIA
160/5.0

Project Name: **Optimus Syria**

Sub Project: **Rotor Hub and Pitch System**

Authors:

Matriculation number:

Dhruvin Bhupatbhai Kakdiya

770612

Adharsh Pappiniseri Veedu

770483

Syed Mohammed Sikandar

770481

Muthu Thirunavukarasu Sivamuthu Manickam

770823

Supervisor:

Prof. Peter Quell

Date: 27.01.2026

Acknowledgements

We would like to express our heartfelt appreciation to our supervisor, Prof. Peter Quell, for his unwavering support, guidance, and insightful expertise throughout the entire OPTIMUS SYRIA project journey. His directions were crucial in helping us reach our objectives.

We also wish to express our sincere gratitude to Prof. Torsten Faber, Mr. Andreas Manjock, Prof. Rajesh Saiju, Prof. Marina Blohm, Prof. Alois Schaffarczyk, Prof. David Schlipf, and Dr. Laurence for their efforts in organizing and facilitating this project. The opportunities they created for collaboration allowed us to work in diverse teams under their knowledgeable guidance. Their expertise and perspectives were tremendous assets that greatly contributed to the project's success.

Lastly, being part of this project as a representative of the Rotor Hub and Pitch System team was an extraordinary experience. It felt like engaging in a real-world project, providing us with invaluable learning opportunities and lasting memories that we will treasure forever.

Table of Contents

Acknowledgements.....	II
List of Abbreviations	V
List Of Symbols	VII
List of Figures	XI
List of Tables	XIII
1. Introduction.....	1
2. Relevant Standards and Guidelines.....	2
2.1 Pitch System.....	2
2.2 Electric Motor	3
2.3 Blade Bearing.....	3
2.4 Lubrication.....	3
2.5 Bolted Connection	4
2.6 Hub and Spinner	4
3. Loads.....	5
4. Engineering Design Framework and Calculations.....	8
4.1 Rotor Hub.....	8
4.1.1 Shapes of the Hub	10
4.1.2 Material of the Hub	12
4.1.3 CAD Design and Dimensions	13
4.2 Pitch System.....	14
4.2.1 Classification of pitch system	14
4.2.2 Comparison between different concepts of pitch systems	14
4.2.2.1 Hydraulic pitch system.....	14
4.2.2.2 Electrical pitch system	15
4.2.3 Electrical Pitch System	16
4.2.3.1 Electric Motor	16
4.2.3.2 Pitch drive selection	19
4.2.3.3 Specification of Motor	23
4.2.3.4 CAD Model of Motor	24
4.2.3.5 CAD Model of Gearbox.....	25
4.2.3.6 Specification of Pitch System	25
4.2.3.7 CAD Model of Pitch Drive Assembly	26
4.2.3.8 Backup Supply System	26
4.4 Blade bearing	30
4.4.1 Types of Bearings	31

4.4.2 Blade attachment.....	33
4.4.3 Dimensioning of the Three-row roller bearing	35
4.4.4 Pitch Bearing Safety Factor Calculation.....	37
4.4.5 CAD Model of Bearing and its Dimensions	43
4.5 Lubrication System	44
4.5.1 Comparison of Manual and Automatic Lubrication	45
4.5.2 Types of Automatic Lubrication Systems.....	45
4.5.3 Grease volume calculation	46
4.5.4 Grease Type Selection	47
4.5.5 Lubrication pump and Reservoir calculation	48
4.5.6 Lubrication Pinion.....	49
4.5.7 CAD Model of Lubrication Pinion	50
4.6 Labyrinth Sealing.....	50
4.7 Spinner	53
4.7.1 CAD Model of Spinner	53
4.8 Stiffening Ring.....	54
4.8.1 CAD Model of Stiffening Ring.....	55
4.9 Complete Assembly of Rotor Hub and Pitch System.....	55
4.10 Part List.....	58
5. External Supporters.....	59
6. Maintenance & Strategies	60
7. Weight and cost.....	62
8. Environmental Life Cycle Assessment	63
9. Project Planning and Task Allocation.....	66
10. Key Takeaways from the Project	69
11. Project Summary and Future Work	70
References.....	71

List of Abbreviations

MW	Mega Watt
GW	Giga Watt
WEC	Wind Energy Converter
IEC	International Electrotechnical Commission
DNV	Det Norske Veritas
ISO	International Organization for Standardization
MPa	Mega Pascal
OEMs	Original Equipment Manufacturers
AC	Alternating Current
DC	Direct Current
IM	Induction Motors
PMSM	Permanent Magnet Synchronous Motors
SynRM	Synchronous AC reluctance motor
PF	Power Factor
U	Voltage
IP	Ingress Protection
DLCs	Design Load Cases
BCD	Bolt Circle Diameter
kN	Kilo Newton
N	Newton
M	Meter
Mm	Millimetre
Kg	Kilo gram

kNm Kilo Newton Meter

KWh Kilo Watt Hour

L Liter

CAD Computer Aided Drawings

SKF Svenska Kullagerfabriken

WTG Wind Turbine Generators

List Of Symbols

F_{xy}	kN	Axial force
F_z	kN/m	Radial force
M_{xy}	kN/m	Bending moment
M_z	kN/m	Pitching torque
M	kN/m	Blade side moment
M_{fric}	kN/m	Friction torque of the pitch bearing
J	kg/m^2	Blade inertia
φ	rad/sec^2	Pitch angular acceleration
f_S	-	Bolt connection factor
W_R	kN/m	Specific friction force
D_L	m	Raceway diameter
k	-	K-factor
f_A	-	Adjacent construction factor
f_L	-	Raceway factor
μ	-	Friction coefficient
mn	-	Gear module
$Df2min$	m	Gear Pitch diameter
Z_{ring}	m	Number of teeth for the ring
Z_{pinion}	-	Number of teeth for the Pinion
$i_{bearing}$	-	Transmission ratio
$i_{gearbox}$	-	Gearbox ratio
M_m	kN/m	Motor torque
$M_{nominal}$	kN/m	Nominal torque
TOL	kN	Overload

$M_{max, gearbox}$	kN/m	Maximum torque for pitch gearbox
$M_{max, bearing}$	kN/m	Maximum torque at bearing's teeth
MB	kN/m	Brake torque
U N	V	Nominal motor voltage
I max	A	Maximum motor current
t	s	Time based on pitch rate
D_{pw}	mm	Bearing raceway diameter
D_w	mm	Bearing roller diameter
L	mm	Roller diameter
Z	mm	Number of Rollers
Q_{max_rigid}	kN	Maximum roller force for ideal conditions
$Q_{max_flexible}$	kN	Flexible roller force for ideal conditions
p_{max}	kN	Max Hertzian pressure
p_{0max}	kN	Ideal Hertzian pressure
$F_{t,12}$	kN	Tangential force on gear
$F_{bn,12}$	kN	Normal force on gear
$F_{rn,12}$	kN	Radial force on gear
α	Degrees	Pressure angle
$F_{t,12_nomi}$	kN	Nominal force on gear
K_a	-	The application factor
K_v	-	Dynamic factor
K_1	-	Gear quality
$K_{H\beta}$	-	Face width factor tooth width on the flank stress
$K_{F\beta}$	-	Face width factor tooth root stress
F_{sh}	μm	Elastic deformations factor
F_{ma}	μm	Manufacturing deviations factor

$F\beta_x$	μm	Effective flank line deviation before running-in
$F\beta_y$	μm	Effective flank line deviation after running-in
N_f	-	Width factor for the tooth root
$KH\alpha$	-	Face load factor
KF_{ges}	-	Tooth base strength factor
Kh_{ges}	-	Tooth flank/pitting factor
σ_{f01}	N/mm^2	The Maximum local tooth stress
Y_{fa}	-	Form factor
Y_{sa}	-	Stress correction factor
Y_{ϵ}	-	Overlap Factor
σ_{f12}	N/mm^2	Total tooth root stress
σ_{fg1}	N/mm^2	Tooth root limit strength
Y_{NT}	-	Service life factor
Y_X	-	Size Factor
S_{f1}	-	Safety of the tooth root load capacity
σ_{H0}	N/mm^2	Flank pressure that occurs at the rolling point
Z_H	-	Zone factor
Z_E	-	Elasticity factor
Z_s	-	Coverage factor
$Z_{\mathfrak{W}}$	-	Screw factor
σ_{HG}	N/mm^2	Flank limit strength
σ_{Hlim}	N/mm^2	Tooth flank fatigue strength
Z_{NT}	-	Service life factor
Z_L	-	Lubricant factor
Z_V	-	Velocity factor
Z_R	-	Roughness factor

ZW	-	Material pairing factor
ZX	-	Size factor
$SH12$	-	Safety of the flank load capacity
Fq_f_ges	kN	Axial force at shaft and hub joint
Fa_f_ges	kN	Lateral force at shaft and hub joint
$Nsin$	-	No. of bolts (inner BCD)
$Nsout$	-	No. of bolts (inner BCD)

List of Figures

Figure 1 : Balde root Co-ordinate system [3]	5
Figure 2 : Welded Steel hub[4]	9
Figure 3 : Castel steel hub [5]	9
Figure 4 : Shape of the Spherical Hub [7]	10
Figure 5 : Shape of the Star-shaped Hub [7].....	11
Figure 6 : Shape of the Star-shaped Hub [8].....	12
Figure 7 : Hub CAD Model of Optimus Syria.....	13
Figure 8 : Hydraulic Pitch system [4]	15
Figure 9 : Electrical Pitch Systems [8]	16
Figure 10 : Typical torque-speed curve of asynchronous induction motors [10]	17
Figure 11 : Typical torque and power-speed characteristic curve of PMSM AC. [13]	18
Figure 12 : Classical torque-speed characteristics of SynRM [15].....	18
Figure 13 : Motor CAD Model of Optimus Syria.....	24
Figure 14 : Gearbox CAD Model of Optimus Syria.....	25
Figure 15 : Pitch Drive Assembly of Optimus Syria	26
Figure 16 : Battery CAD Model of Optimus Syria.....	29
Figure 17 : Inverter CAD Model of Optimus Syria.....	30
Figure 18 : Double row four-point contact ball bearing external toothed [25]	31
Figure 19 : Three raw rollers bearing with internal toothed [25]	32
Figure 20 : Three raw rollers bearing with External toothed,2024 [25]	32
Figure 21 : Three raw ball and roller bearing [27].....	33
Figure 22 : Inner Ring mounted blade,2024 [8]	34
Figure 23 : Outer Ring mounted blade,2024 [28].....	34
Figure 24 : 2 D Sketch of Three-row roller bearing (External teeth)	36
Figure 25 : Forces on Gear[29].....	38
Figure 26 : Bearing CAD Model of Optimus Syria.....	43
Figure 27: Cross-section view of Bearing	44
Figure 28 : SKF Grease [31].....	48
Figure 29 : Lubrication Pump [32]	49
Figure 30 : Lubrication Pinion CAD Model of Optimus Syria	50
Figure 31 : Lubrication pinion engagement with blade bearing ring gear.....	50
Figure 32 : Cross-section view of Lab Sealing of Blade	51
Figure 33 : Spinner Cross-section view Lab Sealing.....	52
Figure 34 : Cross-section view Lab Sealing of Blade.....	52
Figure 35 : Lab Sealing Model	52
Figure 36 : Spinner CAD Model of Optimus Syria	53
Figure 37 : Stiffening Ring CAD Model of Optimus Syria.....	55
Figure 38 : Shaft side view of the complete rotor hub and pitch system assembly of Optimus Syria	56

Figure 39 : Complete rotor hub and pitch system assembly of Optimus Syria	56
Figure 40 : Assembly without spinner	57
Figure 41 : Top Cross-section view Assembly.....	57
Figure 42: View from front side.....	58

List of Tables

Table 1: Loads given by Load team at Blade root	6
Table 2 : Maximum loads extracted from the simulated loads team	6
Table 3 : Final resulting values from the Loads team	6
Table 4 : Loads given by the supervisor	7
Table 5 : Loads given by load team at Pitch Bearing	7
Table 6 : Mechanical Properties of Spherical Cast Iron (EN-GJS-400-18).....	13
Table 7 : Specification of rotor hub	13
Table 8 : Specification of Motor	23
Table 9 : Specification of the Pitch System	25
Table 10 : Specification of Battery [22]	29
Table 11 : Specification of Inverter [23]	30
Table 12 : Specification of Bearing	43
Table 13 : Comparison of Manual and Automatic Lubrication[30].....	45
Table 14 : Comparison of Automatic Lubrication Systems [30]	45
Table 15 : Specification of Lubrication Pinion [33]	49
Table 16 : Specification of Stiffening Ring	55
Table 17 : Part List.....	58
Table 18 : Weight and Cost of all the Components.....	62
Table 19 : Co ₂ Emission from the Components lifecycle	65

1. Introduction

Syria holds promising potential for the development of renewable energy resources, particularly wind energy, due to its diverse geography and favourable wind conditions in several regions. In the context of increasing energy demand and the need for sustainable and resilient power systems, wind energy represents a viable solution to enhance energy security, reduce reliance on conventional energy sources, and minimize environmental impacts. The expansion of wind power also supports long-term economic development and aligns with global efforts toward cleaner energy systems.[1]

In line with these objectives, the OPTIMUS SYRIA project focuses on the conceptual design of an onshore wind turbine adapted to local environmental and operational conditions. The project aims to achieve efficient and reliable power generation while emphasizing system simplicity, cost-effectiveness, and environmental responsibility. Key considerations include compliance with international design standards, reduction of carbon emissions, and the use of durable and recyclable materials to ensure sustainable turbine operation throughout its lifecycle.

To successfully realize these goals, the OPTIMUS SYRIA project is organized into several specialized sub-teams, each responsible for the design and analysis of a specific wind turbine subsystem. These teams cover a broad range of disciplines, including project management, aerodynamic and structural components, electrical systems, control strategies, and mechanical drivetrain elements. This structured and collaborative approach ensures effective integration of all subsystems and contributes to the overall performance and reliability of the wind turbine.

As part of the Optimus Syria project, our team is responsible for the design of the Rotor Hub and Pitch System, which plays a crucial role in controlling turbine power output and ensuring safe operation under varying wind conditions. The team focuses on achieving a reliable and efficient pitch mechanism while maintaining close coordination with related subsystem teams to ensure mechanical compatibility and smooth system integration. This cooperation is essential for the successful implementation of the overall wind turbine design.

2. Relevant Standards and Guidelines

The design of Wind turbines must achieve certain objectives, such as ensuring regular operational conditions, safeguarding personnel and equipment, and minimizing risks to human life. The structures and components should meet their expected lifespan, and the overall system must demonstrate a sufficient level of reliability.

To meet these goals, wind turbines must be designed according to standards that provide principles, technical requirements, and guidelines for the design and manufacturing of machinery components and structures for wind turbines. These standards ensure safety and performance in both ultimate and serviceability limit states.

For our project the Optimus Syria, we are following DNV standards. ‘Machinery for wind turbines – DNV was consulted to establish standards for designing the Rotor hub and Pitch system components. The design requirements for components are outlined below.

2.1 Pitch System

For pitch systems incorporating a pitch gearbox, the structural assessment shall cover critical components, including the pitch gearbox teeth and the blade bearing teeth. The evaluation must account for fatigue loading as well as static strength checks against tooth root failure and surface pitting, in accordance with the requirements specified in Section 7.2.2.1 [2].

The determination of loads acting on the blade pitch mechanism shall be based on the design load cases defined in Section 4 of DNV-ST-0437.

When a pitch gearbox is employed, the load capacity analysis of both the gearbox and pitch gear teeth shall follow the ISO 6336 series. In addition to fatigue verification, a static strength assessment shall be performed to confirm resistance to tooth breakage and pitting, ensuring compliance with the prescribed safety factors. For pitting resistance, safety factors of 1.0 are required for both gearbox teeth and pitch system teeth. For tooth root strength, the minimum safety factors are specified as 1.1 for gearbox teeth and 1.2 for pitch system teeth, as outlined in Section 7.4.2.1 [2].

For bearings used in pitch and yaw actuators, the static safety factor S_0 , determined in accordance with ISO 76:2006, shall not be less than 1.1, as specified in Section 6.5.1.4 [2].

Locking mechanisms shall be designed such that, even in the absence of an active brake, they are capable of reliably preventing any unintended rotation of the rotor, nacelle, or rotor blades. Both the engaged (locked) and disengaged (unlocked) positions of the locking devices must be secured against accidental activation or release, in compliance with Section 7.5 [2].

2.2 Electric Motor

Electric motors shall be designed based on the expected operating durations and thermal conditions. The selected duty types and performance characteristics shall comply with the requirements specified in IEC 60034-1, "Rating and Performance."

The nominal torque and the equivalent (reference) torque of auxiliary drives, such as pitch motors, shall be consistent with the results obtained from the corresponding load calculations. In addition, the design and selection of electric motors shall conform to the general machinery requirements defined in DNVGL-ST-0361 for wind turbine components.

2.3 Blade Bearing

Blade and yaw bearings are predominantly subjected to small oscillatory motions rather than continuous rotation. For this reason, their static load rating shall be determined directly from the maximum contact stress occurring between the rolling elements and the raceways. The permissible Hertzian contact stress must be defined by the bearing manufacturer, taking into account factors such as material properties, surface hardness, and hardening depth. This information shall be documented within the design calculations.

The static safety factor for blade and yaw bearings is defined as the ratio between the maximum allowable Hertzian contact stress and the calculated maximum contact stress. This factor shall be at least 1.1, in accordance with Section 6.5.1.3 [2].

According to ISO 76:2006, the maximum permissible Hertzian contact stress for roller bearings shall not exceed 4000 MPa.

2.4 Lubrication

A continuous and reliable supply of lubricant must be ensured for the blade bearing gear teeth and the rolling contact surfaces throughout all operating conditions of the wind turbine.

A dedicated lubrication system shall be provided for the bearing teeth, and its proper functionality must be documented. If required, system performance may be verified through periodic test runs, typically conducted once every 24 hours. During these tests, the rotor blades and blade bearings shall be rotated to guarantee sufficient relubrication.

Suitable collection reservoirs shall be installed to manage excess lubricant discharged from blade bearing components, in accordance with Section 7.4.2.12 [2].

2.5 Bolted Connection

Analytical calculations of axially loaded bolted joints should be performed on the basis of VDI 2230 or other widely recognized design codes and analytical methodologies.

2.6 Hub and Spinner

For rotor hubs, spheroidal graphite cast iron (EN-GJS) in accordance with EN 1563:2012-03 may be used, provided that the required mechanical properties are satisfied.

Without additional verification, cast iron materials exhibiting a fracture elongation $A < 12.5\%$ or an impact energy $K_{v,\text{mean}} < 10 \text{ J}$ (mean value of three tests) shall not be used for components that are critical for force transmission and are subjected to high dynamic loading, such as the rotor hub.

Requirements related to manufacturing processes—including material selection, bonding techniques, laminate construction, curing duration, resin application, and surface finishing—for nacelle covers and spinners made of fibre-reinforced plastics (FRP) shall comply with Section 5 of DNV-ST-0376.

Spinner areas that present a risk of falling from height or slipping shall be equipped with appropriate safety attachment points, as specified in Section 11.2.5 [2].

3. Loads

Load Definition and Load Basis

The structural design of the rotor hub, blade bearing, and pitch system requires a clear definition of the governing loads acting at the blade root and hub interface. These loads originate from aerodynamic forces, gravitational effects, inertial contributions, and control actions during turbine operation. To ensure a conservative and reliable design, load values are derived from simulation results and validated against reference loads from comparable wind turbine configurations.

Blade Root Load Components

Load simulations were carried out by the load analysis team to determine the extreme forces and moments acting at the blade root. The resulting peak values were extracted from the simulated load cases and expressed in the blade root coordinate system. This coordinate system defines three orthogonal force components and three corresponding moment components acting at the blade–hub interface.

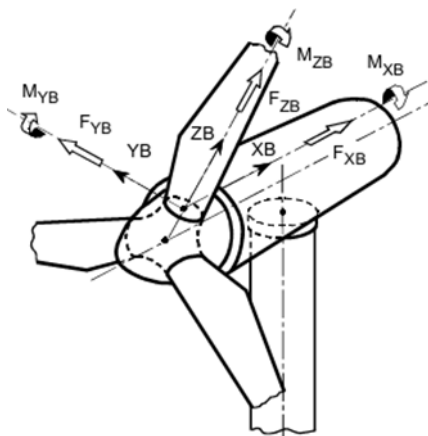


Figure 1 : Balde root Co-ordinate system [3]

The force components F_x , F_y , and F_z represent loads acting along the principal axes of the blade root coordinate system. In addition, the moment components M_x , M_y , and M_z describe bending and torsional effects acting on the blade root. These load components are illustrated schematically in the blade root coordinate system shown in Figure 1.

The extracted maximum load values obtained from the simulation results are summarized in Table 3.1. These values represent extreme loading conditions and serve as an upper bound for structural assessment.

Parameter	Type	File Name	DLC Name	Calculated Extreme	RootFxb1 (kN)	RootFyb1 (kN)	RootFzb1 (kN)	RootMxb1 (kNm)	RootMyb1 (kNm)	RootMzb1 (kNm)	RootFxyb1 (kN)	RootMxyb1 (kNm)	Time (sec)	Wind1Vex (m/sec)
RootFxb1	Minimum	\Data\ DLC6.1\ DLC6.1.1.out	DLC_6.1	-1.100E+003	-1.100E+003	-7.009E+001	-2.214E+002	1.354E+003	-3.474E+004	8.374E+002	1.102E+003	3.476E+004	2.669E+002	4.240E+001
RootFxb1	Maximum	\Data\ DLC6.1\ DLC6.1.3.out	DLC_6.1	1.153E+003	1.153E+003	-4.323E+002	-1.913E+002	1.232E+004	3.505E+004	-1.041E+003	1.231E+003	3.715E+004	4.494E+002	5.098E+001
RootFyb1	Minimum	\Data\ DLC4.2\ DLC4.2.23.6.out	DLC_4.2	-1.238E+003	4.766E+002	-1.238E+003	1.723E+003	4.116E+004	3.587E+003	4.203E+002	1.327E+003	4.132E+004	2.086E+002	2.765E+001
RootFyb1	Maximum	\Data\ DLC4.2\ DLC4.2.23.6.out	DLC_4.2	1.267E+003	-3.645E+002	1.267E+003	1.254E+003	-4.577E+004	-9.474E+003	-1.558E+003	1.318E+003	4.674E+004	2.116E+002	2.244E+001
RootFzb1	Minimum	\Data\ DLC6.1\ DLC6.1.3.out	DLC_6.1	-5.890E+002	-6.387E+001	-4.720E+001	-5.890E+002	2.614E+003	3.980E+003	-8.809E+001	7.941E+001	4.761E+003	2.772E+002	4.089E+001
RootFzb1	Maximum	\Data\ DLC1.2\ DLC1.2.25.2.out	DLC_1.2	3.252E+003	5.399E+002	1.174E+002	3.252E+003	-4.637E+003	1.187E+004	-1.354E+002	5.525E+002	1.274E+004	1.421E+002	3.069E+001
RootMxb1	Minimum	\Data\ DLC4.2\ DLC4.2.23.6.out	DLC_4.2	-4.577E+004	-3.645E+002	1.267E+003	1.254E+003	-4.577E+004	-9.474E+003	-1.558E+003	1.318E+003	4.674E+004	2.116E+002	2.244E+001
RootMxb1	Maximum	\Data\ DLC4.2\ DLC4.2.23.6.out	DLC_4.2	4.243E+004	4.822E+002	-1.134E+003	7.926E+002	4.243E+004	6.861E+003	-1.600E+002	1.232E+003	4.298E+004	2.147E+002	2.323E+001
RootMyb1	Minimum	\Data\ DLC6.1\ DLC6.1.1.out	DLC_6.1	-3.506E+004	-1.098E+003	-8.428E+001	-2.788E+002	2.388E+003	-3.506E+004	1.010E+003	1.102E+003	3.514E+004	2.675E+002	3.932E+001
RootMyb1	Maximum	\Data\ DLC6.1\ DLC6.1.3.out	DLC_6.1	3.517E+004	1.118E+003	-2.232E+002	-2.303E+002	6.604E+003	3.517E+004	-6.845E+002	1.140E+003	3.578E+004	4.047E+002	4.835E+001
RootMzb1	Minimum	\Data\ DLC6.1\ DLC6.1.4.out	DLC_6.1	-1.665E+003	7.169E+002	-6.865E+002	-5.756E+002	2.098E+004	2.419E+004	-1.665E+003	9.925E+002	3.202E+004	4.560E+002	4.316E+001
RootMzb1	Maximum	\Data\ DLC6.1\ DLC6.1.1.out	DLC_6.1	1.594E+003	-8.232E+002	-1.816E+002	-5.435E+002	6.998E+003	-2.835E+004	1.594E+003	8.430E+002	2.920E+004	6.167E+002	5.357E+001
RootFxyb1	Minimum	\Data\ DLC4.2\ DLC4.2.15.1.out	DLC_4.2	4.935E-001	-2.782E-001	-4.076E-001	-5.690E+002	1.702E+002	7.119E+002	-5.500E+000	4.935E-001	7.319E+002	4.515E+002	1.497E+001
RootFxyb1	Maximum	\Data\ DLC4.2\ DLC4.2.23.6.out	DLC_4.2	1.327E+003	4.766E+002	-1.238E+003	1.723E+003	4.116E+004	3.587E+003	4.203E+002	1.327E+003	4.132E+004	2.086E+002	2.765E+001
RootMxyb1	Minimum	\Data\ DLC4.2\ DLC4.2.17.3.out	DLC_4.2	1.008E+001	-4.734E-001	7.790E+000	-5.659E+002	1.006E+001	7.430E-001	-3.020E+000	7.804E+000	1.008E+001	3.515E+002	1.754E+001
RootMxyb1	Maximum	\Data\ DLC4.2\ DLC4.2.23.6.out	DLC_4.2	4.674E+004	-3.645E+002	1.267E+003	1.254E+003	-4.577E+004	-9.474E+003	-1.558E+003	1.318E+003	4.674E+004	2.116E+002	2.244E+001

Table 1: Loads given by Load team at Blade root

Fx (kN)	Fy(kN)	Fz(kN)	Mx (kNm)	My(kNm)	Mz(kNm)
1153 KN	1267 KN	3252 KN	4243 KN	3517 KN	1594 KN

Table 2 : Maximum loads extracted from the simulated loads team

Interpretation of Force and Moment Components

Among the extracted load components, the bending moments play a dominant role in the structural design of the blade bearing and pitch system. The moment M_x corresponds to the edgewise bending moment, while M_y represents the flapwise bending moment acting on the blade. The torsional moment M_z is associated with pitching torque and directly influences the sizing of pitch system components.

For design purposes, the force components acting in the axial directions can be combined to obtain a resultant axial force at the blade root. Similarly, the bending moments about orthogonal axes are combined to form an equivalent resultant bending moment. These resultant values provide a simplified and conservative representation of the load state, which is suitable for preliminary component sizing.

The resulting combined forces and moments derived from the simulation data are presented in Table 3.2

Axial Force (Fxy)	Radial force (Fz)	Bending Moment	Pitching Torque (Mz)
1327 KN	3252 KN	4674 KN	1594 KN

Table 3 : Final resulting values from the Loads team

Selection of Design Loads for Component Sizing

Although the simulated loads represent extreme operating conditions, their direct application in the detailed design of pitch system components and blade bearings would result in oversized and economically unfavourable designs.

For this reason, the final design of the pitch system and blade bearing is based on reference load values provided by the project supervisor. These loads were derived from a wind turbine of comparable size and operational characteristics and are considered representative of the intended application. The selected design loads ensure a balanced approach between structural safety, manufacturability, and cost efficiency.

The adopted design loads for the pitch system components are listed in Table 4.

Fx (kN)	Fy(kN)	Fz(kN)	Mx (kNm)	My(kNm)	Mz(kNm)	Axial Force	Bending Moment (Fxy)
							(Mxy)
840 KN	630 KN	650 KN	17000 KNm	36000 KNm	370 KN	730 KN	30000 KNm

Table 4 : Loads given by the supervisor

Parameter	Type	File Name	DLC Name	Calculated Extreme	RootFx1 (kN)	RootFy1 (kN)	RootMx1 (kNm)	RootMy1 (kNm)	YawBrFxp (kN)	YawBrMxp (kNm)	LSShftFxy1 (kN)	LSShftMxy1 (kNm)	Time (sec)	Wind1VelX (m/sec)
RootFx1	Minimum	\Data\DL6.1\DL6.1_4.out	DLC.6.1	-5.779E+002	-5.779E+002	-4.088E+002	1.237E+004	1.658E+004	7.969E+002	3.622E+004	1.693E+003	2.449E+004	4.567E+002	4.897E+001
RootFx1	Maximum	\Data\DL1.2\DL1.2_25_2.out	DLC.1.2	5.711E+002	5.711E+002	2.198E+002	-5.055E+003	1.650E+004	8.377E+002	5.615E+003	2.448E+003	1.287E+004	1.389E+002	3.155E+001
RootFy1	Minimum	\Data\DL4.2\DL4.2_23_6.out	DLC.4.2	-9.660E+002	-1.821E+002	-9.660E+002	2.734E+004	-1.377E+004	-1.756E+002	-6.354E+003	3.367E+003	2.970E+004	2.086E+002	2.765E+001
RootFy1	Maximum	\Data\DL4.2\DL4.2_23_6.out	DLC.4.2	9.341E+002	2.412E+002	9.341E+002	-3.137E+004	1.135E+004	-4.784E+002	-1.131E+004	3.172E+003	2.850E+004	2.117E+002	2.331E+001
RootMx1	Minimum	\Data\DL4.2\DL4.2_23_6.out	DLC.4.2	-3.184E+004	3.133E+002	9.247E+002	-3.184E+004	1.357E+004	-5.192E+002	-1.217E+004	3.213E+003	3.308E+004	2.116E+002	2.244E+001
RootMx1	Maximum	\Data\DL4.2\DL4.2_23_6.out	DLC.4.2	2.799E+004	-2.066E+002	-8.906E+002	2.799E+004	-1.445E+004	-1.751E+002	3.356E+003	3.102E+003	2.792E+004	2.148E+002	2.345E+001
RootMy1	Minimum	\Data\DL6.1\DL6.1_4.out	DLC.6.1	-1.663E+004	-5.755E+002	-3.953E+002	1.177E+004	-1.663E+004	7.922E+002	3.472E+004	1.702E+003	2.337E+004	4.568E+002	4.865E+001
RootMy1	Maximum	\Data\DL1.2\DL1.2_9_6.out	DLC.1.2	1.888E+004	5.478E+002	-4.591E+002	1.097E+004	1.888E+004	1.403E+003	7.532E+003	2.768E+003	8.423E+003	5.163E+002	9.501E+000
YawBrFxp	Minimum	\Data\DL5.1\DL5.1_8_6.out	DLC.5.1	-1.324E+003	-1.880E+002	-1.815E+002	1.922E+003	-6.411E+003	-1.324E+003	-8.502E+003	1.535E+003	9.109E+003	2.081E+002	7.595E+000
YawBrFxp	Maximum	\Data\DL6.1\DL6.1_6.out	DLC.6.1	1.667E+003	-2.948E+002	-3.643E+002	1.389E+004	-7.545E+003	1.667E+003	-1.708E+003	4.450E+002	1.072E+004	6.098E+002	5.370E+001
YawBrMxp	Minimum	\Data\DL6.1\DL6.1_1.out	DLC.6.1	-2.836E+004	1.716E+002	-5.831E+002	1.667E+004	7.122E+003	8.728E+002	-2.836E+004	2.900E+003	1.494E+004	2.396E+002	4.607E+001
YawBrMxp	Maximum	\Data\DL6.1\DL6.1_1.out	DLC.6.1	4.236E+004	-5.495E+002	-5.444E+002	1.797E+004	-1.434E+004	7.667E+002	4.236E+004	1.715E+003	2.949E+004	4.564E+002	5.030E+001
LSShftFxy1	Minimum	\Data\DL6.1\DL6.1_4.out	DLC.6.1	4.607E+000	-1.678E+002	1.108E+002	-2.212E+003	-7.925E+003	-1.621E+002	-2.133E+003	4.607E+000	1.505E+004	2.690E+002	4.050E+001
LSShftFxy1	Maximum	\Data\DL4.2\DL4.2_15_1.out	DLC.4.2	3.630E+003	1.310E+002	8.215E+002	-2.825E+004	6.865E+003	-2.777E+002	-3.974E+003	3.630E+003	8.749E+003	2.157E+002	2.060E+001
LSShftMxy1	Minimum	\Data\DL4.2\DL4.2_23_6.out	DLC.4.2	2.723E+000	3.237E+001	-4.182E+002	9.797E+003	7.697E+002	3.000E+001	-1.535E+001	2.659E+003	2.723E+000	4.118E+002	3.679E+000
LSShftMxy1	Maximum	\Data\DL4.2\DL4.2_23_6.out	DLC.4.2	3.538E+004	3.549E+002	8.827E+002	-3.096E+004	1.481E+004	-5.716E+002	-1.226E+004	3.252E+003	3.538E+004	2.116E+002	2.392E+001

Table 5 : Loads given by load team at Pitch Bearing

4. Engineering Design Framework and Calculations

4.1 Rotor Hub

The rotor hub is the first main component of the mechanical drivetrain of a wind turbine. Although it is part of the rotor, it is closely connected to the drivetrain in both function and structure. The hub is used to attach the rotor blades to the main shaft and to transfer the rotational energy produced by the blades to the drivetrain. In pitch-controlled wind turbines, the hub also contains the blade pitch system, which allows the blade angles to be adjusted in order to improve energy capture and control turbine operation under different wind conditions.

The rotor hub is one of the most highly loaded components in a wind turbine because all rotor forces and moments act at this single point. Therefore, the choice of material is very important to ensure sufficient strength and long service life. Detailed strength calculations and careful sizing are required to avoid high local stresses and possible structural failure.

In general, three main material and design options are used for rotor hubs:

- Welded sheet steel
- Cast steel
- Forged steel

Welded Sheet steel

Welded sheet steel hubs are produced by joining individual steel plates into a hub shell with welded seams. In early turbine generations, this offered flexibility in fabrication with low tooling requirements. However, weld joints act as stress risers under cyclic loading, which limits fatigue performance in large turbines. [4]

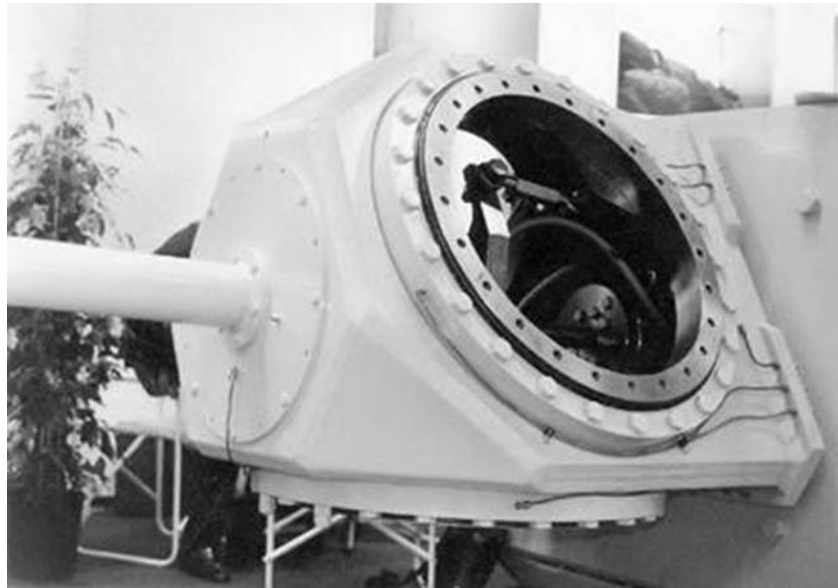


Figure 2 : Welded Steel hub[4]

Cast Steel

Cast hubs, typically formed from cast steel or cast iron (such as spheroidal graphite cast iron (EN-GJS)), allow near-net-shape geometries with smoother load paths and reduced welding stresses. Casting is widely used for large structural parts, including hubs, as discussed by NREL.[5]



Figure 3 : Castel steel hub [5]

Forged Steel

Forged steel components exhibit improved mechanical properties due to grain flow alignment and reduced internal defects. Though specific hub forgings are uncommon in large turbines, analogous research on forged rotor shafts highlights significant strength and fatigue performance advantages over cast components.

4.1.1 Shapes of the Hub

For cast hubs in modern wind turbines, several geometric configurations have been developed to efficiently transfer blade loads to the main shaft while minimizing stress concentrations and material usage. Among these, three hub shapes are most commonly discussed in literature and industrial practice: the spherical hub, the star-shaped hub, and the topologically optimized hub.

Spherical Hubs

The spherical hub represents one of the earliest geometric concepts used in wind turbine hub design. Its nearly uniform curvature allows loads from the blades to be distributed relatively evenly throughout the structure. The spherical form is advantageous from a stress distribution perspective, as it avoids sharp corners and sudden changes in geometry. However, this design typically requires a larger material volume to achieve the required strength, resulting in higher weight. In addition, manufacturing spherical hubs is more complex due to the curved internal geometry, and access for maintenance and assembly of internal components can be limited.[7]

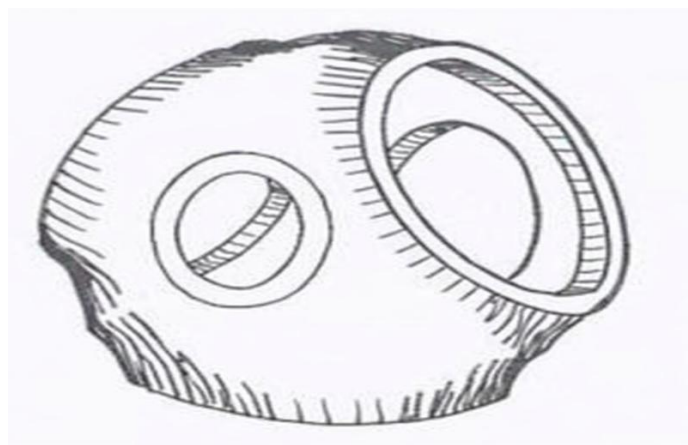


Figure 4 : Shape of the Spherical Hub [7]

Star-shaped Hubs

The star-shaped hub is currently one of the most widely used designs in modern wind turbines. In this configuration, the blade attachment arms extend outward in a star-like arrangement, providing more direct load paths from each blade root to the hub centre and main shaft.

This geometry allows for improved structural efficiency, as material is concentrated along the principal load directions. Compared to spherical hubs, star-shaped hubs generally have lower weight and simpler internal geometry, which facilitates manufacturing, machining, and inspection. Furthermore, maintenance access to blade bearings and pitch system components is improved. Due to these advantages, the star-shaped hub has become a proven and cost-effective solution for large onshore and offshore wind turbines.[7]

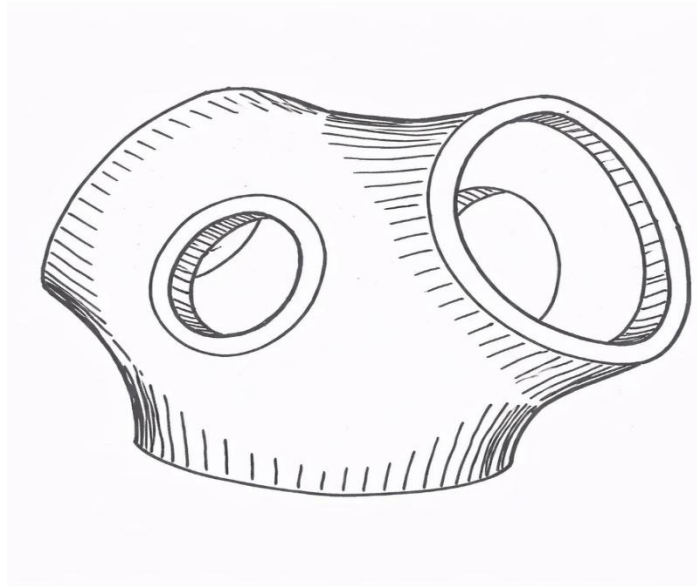


Figure 5 : Shape of the Star-shaped Hub [7]

Topologically Optimized Hub

Topologically optimized hubs represent the most advanced stage of hub shape development. These designs are generated using numerical optimization methods that remove unnecessary material while maintaining required strength and stiffness. The resulting geometry often appears irregular and organic, closely following the actual load paths within the hub.

The main advantage of topologically optimized hubs is significant weight reduction without compromising structural performance. Reduced mass leads to lower loads on the main shaft and drivetrain, improving overall turbine reliability. However, such complex geometries increase manufacturing complexity and may require advanced casting techniques and extensive quality control.

As a result, topologically optimized hubs are still mainly used in research studies or limited industrial applications where performance benefits justify the added cost.[7]

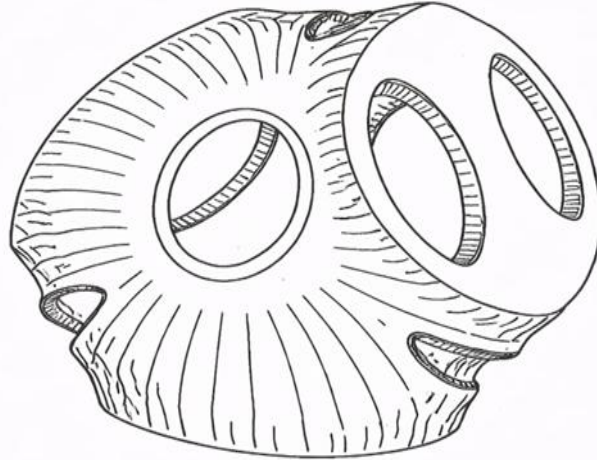


Figure 6 : Shape of the Star-shaped Hub [8]

Overall, The Star Shape Hub emerges as the clearly superior design for the Optimus Syria project. Its primary advantages lie in its high structural simplicity and ease of manufacturing, as it is simpler to cast, weld, and machine than spherical alternatives. Furthermore, the star shape offers easier maintenance access to blade root joints, a lighter overall weight, and lower costs related to materials and labour. These practical benefits make it the most suitable and proven choice for onshore applications.

4.1.2 Material of the Hub

For wind turbine hubs, spheroidal cast iron (EN-GJS-400-18) is an ideal material because of its remarkable strength and ductility, which enable it to effectively bear both high and cyclic stresses. Its robust fatigue resistance guarantees long-term endurance, and the cost-effective casting method makes it easier to create complex hub designs. Furthermore, the material's moderate corrosion resistance makes it ideal for harsh environmental conditions, and its outstanding machinability simplifies precision manufacture. These advantages make it a dependable and affordable choice for hub construction, especially when combined with its proven track record in wind turbine applications.

Spherical Cast Iron (EN-GJS-400-18)		Value
Tensile Strength		360 MPa
Compressive Strength		275 MPa
Yield Strength		220 MPa
Young's Modulus		169 GPa
Density		7100 Kg/m3
Poisson's ratio		0.28

Table 6 : Mechanical Properties of Spherical Cast Iron (EN-GJS-400-18)

4.1.3 CAD Design and Dimensions

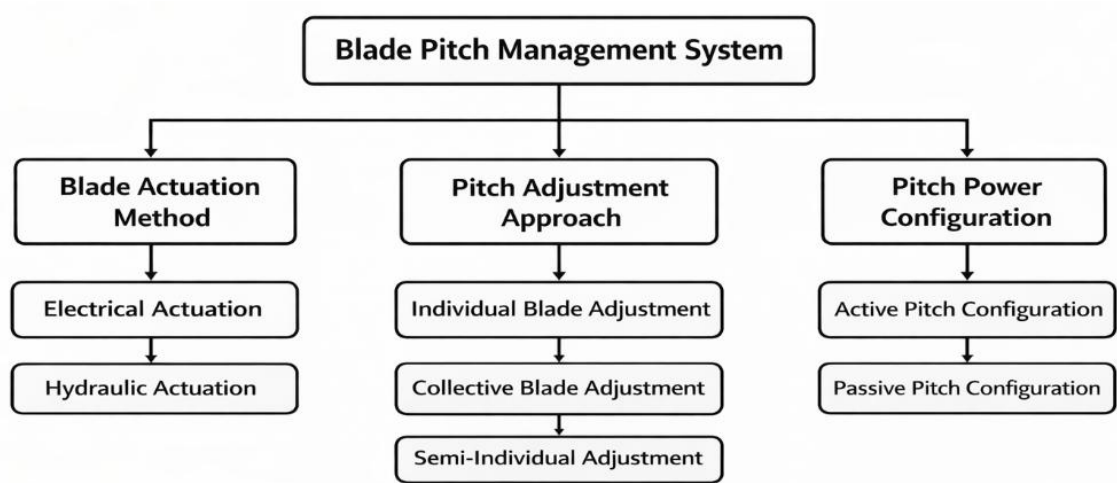
Rotor Hub	Parameters
Hub diameter	4500 mm
Cone angle	4°
Total weight	35 T
Material	EN-GJS-400-18
Hub to shaft BCD	2450 mm (outer) 2250 mm (Inner)
Bolts on inner BCD	94 × M36
Bolts on outer BCD	102 × M36
Hub length	3500 mm

Table 7 : Specification of rotor hub*Figure 7 : Hub CAD Model of Optimus Syria*

4.2 Pitch System

In existing wind turbine technology, all wind turbines are equipped with rotors that utilize blade pitch control called the ‘Pitch System’. This mechanism serves several purposes. The first is to regulate the blade pitch angle, which is essential for controlling the rotor’s power output and speed. Typically, a pitching range of 20 to 25 degrees is sufficient to achieve this. This operation functions in case of power optimization, power limitation, and sound operation modes. The mechanism has a secondary function that significantly impacts its design. To enable the aerodynamic braking of the rotor, the blades must be able to pitch to a feathered position. This requirement expands the pitching range to approximately 90 degrees to stop the wind turbine as well as to protect it from the over speeding in extreme weather conditions. Additionally, it aids in reducing the load on the turbine by adjusting the angles of individual blades. [4]

4.2.1 Classification of pitch system



4.2.2 Comparison between different concepts of pitch systems

Modern wind turbines commonly use either hydraulic or electric pitch systems, which will be discussed in the following sections.

4.2.2.1 Hydraulic pitch system

The hydraulic pitch system works by continuously supplying hydraulic pressure from a power unit. The fluid is transported to the hub via a hollow shaft and a rotating lead-through. The pitch controller

controls valves in the hub to supply hydraulic fluid to the pistons, which extend and retract to change the pitch of the rotor blades. Hydraulic fluid is kept in pressure tanks inside the hub for safety, which enables the blades to shift into a feathered configuration in an emergency. In these circumstances, the piston is driven to position the blades safely as depicted in the picture by a valve that releases the fluid that has been accumulated. [4]

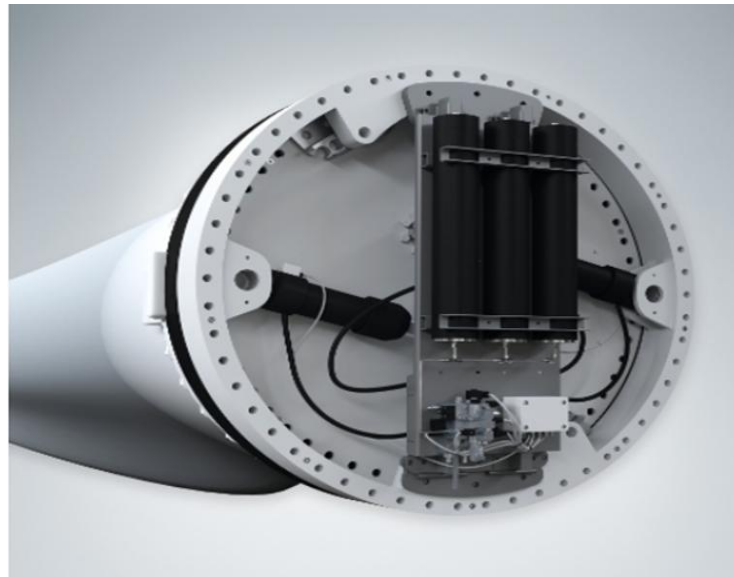


Figure 8 : Hydraulic Pitch system [4]

The hydraulic system offers the benefits of high-power output with small components, high reliability, reduced parts (no gears), no backlash, and no tooth lubrication, but it also comes with the potential for fluid leakage, greater maintenance needs, lower efficiency, and greater energy consumption due to the pump operating constantly. Further, operating costs are high due to ongoing maintenance, replacement of cylinder seals, tubes every 5–10 years, and periodic oil and filtration replacements.[8]

4.2.2.2 Electrical pitch system

Modern MW-class wind turbines use Electric pitch systems with a planetary gear directly attached to the motor are used in contemporary MW-class wind turbines. The pinion wheel rotates the blade's gear ring as a result of the torque from the motor being transferred through the gear. The planetary gear modifies the motor's speed to correspond with the pitch system's low rotational speed while lowering the high torque needed to move the blade. Each pitch motor has its own power storage device, such as capacitors or lithium-ion batteries, to guarantee operation during blackouts. [4]



Figure 9 : Electrical Pitch Systems [8]

The electrical system offers significant advantages, including high efficiency with quick responses, low maintenance requirements, and quiet operation, making it ideal for environments sensitive to noise. However, its complexity, higher chance of failure, and the need for gear lubrication are some drawbacks.[8]

4.2.3 Electrical Pitch System

The electric pitch system in a wind turbine consists of several key components that work together to adjust the blade pitch angle for optimal performance and safety. At its core is the electric pitch motor, pitch drive, and back-up system.

4.2.3.1 Electric Motor

Fundamentally, two types of electric motors are available for the pitch actuator of wind turbines: AC and DC, both of which have their pros and cons. Generally, AC motors are cheaper and require less maintenance, which is why they are more common in current designs. On the other hand, DC motors are more expensive but can be directly powered by an emergency power supply without requiring an additional converter.

However, we briefly investigate all available types and, based on the project priorities, choose the one that best matches.

a) Asynchronous induction Motors (**IM**):

The conventional three-phase AC induction motor is a constant-speed motor that can be easily used in variable-speed applications, albeit typically with reduced efficiency. [9] The squirrel cage rotor induction motor (IM) has low starting torque and a high starting current.

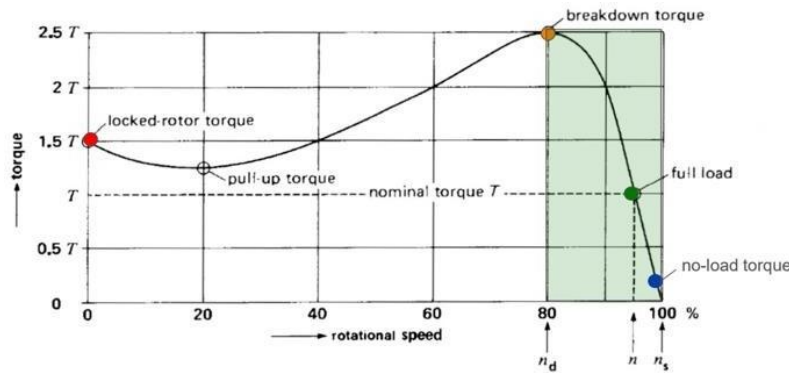


Figure 10 : Typical torque-speed curve of asynchronous induction motors [10]

The torque of an IM is directly proportional to the product of the flux per pole, the rotor current, and the rotor's power factor. The maximum torque, also known as the breakdown torque, depends on the rotor reactance per phase at standstill and is independent of the rotor resistance per phase. However, the speed, or slip, at which it occurs is determined by the rotor resistance per phase. [11]

b) Permanent Magnet Motors

The permanent-magnet synchronous motor (**PMSM**) offers numerous advantages over other types of machines traditionally used for AC servo drives. It has a higher torque-to-inertia ratio and greater power density compared to an induction motor or a wound rotor synchronous motor. This makes it suitable for applications such as robotics and aerospace actuators.

However, it is challenging to control due to its nonlinear dynamic behaviour and time-varying parameters. [12]

Unlike induction motors, the torque-speed characteristic of a **PMSM** does not involve slip, as the rotor is synchronized with the stator's magnetic field. Instead, torque is controlled directly by regulating the I_q component of the stator current.

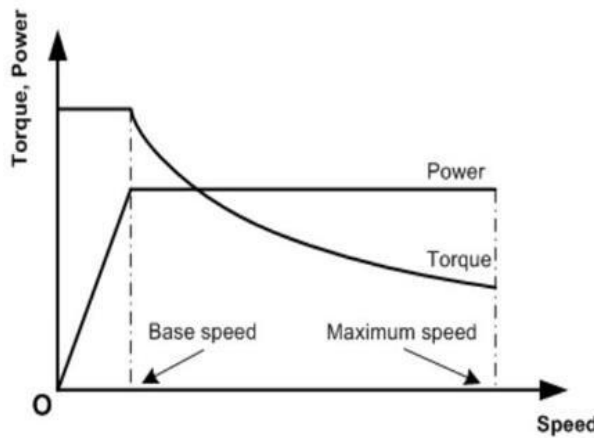


Figure 11 : Typical torque and power-speed characteristic curve of PMSM AC. [13]

c) Synchronous AC reluctance motor (*SynRM*)

The rotor design of a *SynRM* distinguishes it from its *IM* and *PMSM* counterparts. Compared to these conventional motors, *SynRM* achieves higher reliability and easier maintenance (due to very low winding and bearing temperatures, as well as the absence of a cage or *PMs* in the rotor structure), lower cost (due to the lack of *PMs* compared to *PMSM*), faster dynamic response (due to its smaller size within the same power range and lower moment of inertia), a higher speed range (due to wide constant-power operation compared to *IM*), and higher efficiency within the same power range and frame size (due to cold rotor operation compared to *IM*, and higher power density and torque per ampere compared to *IM*). In this sense, *SynRM* offers the high performance of *PMSM* while remaining as inexpensive, simple, and service-friendly as *IM*. [14]

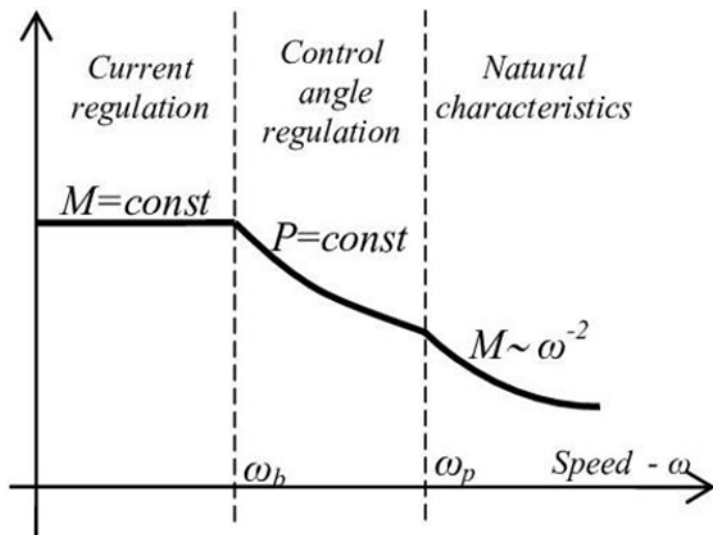


Figure 12 : Classical torque-speed characteristics of SynRM [15]

d) Direct Current DC motors

The *DC* motor consists of a stator and a rotating part, the armature, separated by an air gap. The armature is wound with coils that are connected to a commutator. During rotation, the polarity of the armature winding is changed through the sliding contacts (carbon brushes) running on the commutator, thereby generating constant torque.

If *DC* motors are used in applications requiring relatively high positioning accuracy, servo technology can be integrated into the *DC* machines. The additional module required for this is an encoder system, which can take the form of a resolver, an incremental encoder, or, more commonly, an absolute encoder. This enables the exact speed of the motor to be measured and the precise position of the armature to be determined. [16]

4.2.3.2 Pitch drive selection

In this project, the design priorities are cost, reliability, and low weight. In terms of cost, asynchronous induction motors (*IM*) and synchronous *AC* reluctance motors (*SynRM*) are more favourable. However, as mentioned earlier, *SynRM* offers higher performance compared to *IM*. Therefore, *SynRM* has been chosen for this project.

Pitch actuator static calculation:

In the pitch actuator calculation procedure, torque and rotational speed are two important parameters that should be investigated. Additionally, regarding torque, we first calculate the required torque on the blade side. Then, we examine whether the selected pitch actuator from the market can fulfil the required torque as well as the rotational speed.

Required Torque on the Blade side

However, the required torque on the blade side consists of three parts, the acting wind torque (M_z), the friction torque of the pitch bearing (M_{fric}), and the torque obtained from blade inertia (J). The relevant equation is shown in 1.1. and $\ddot{\varphi}$ is pitch angular acceleration [17]

$$M = M_z + M_{fric} + J \cdot \ddot{\varphi}$$

The inertia of blade about the pitch axis is J [kg/m^2], and the pitch angular acceleration is $\ddot{\varphi}$ [rad/sec^2]. While the desired pitch angular speed is assumed to be 2 deg/sec.

$$2 \text{ deg/sec} \times \pi / 180 \times \pi / 90 \text{ rad/sec} \approx 0.0349 \text{ rad/sec}$$

The friction of the pitch bearing comes with highest uncertainty; it depends on the type of bearing, the number of rolling elements, and the lubrication system. Which in Optimus Syria the pitch bearing is a three-row roller bearing [17]

However, to estimate the friction torque of the pitch bearing, we have used equations provided by bearing manufacturer. The overall friction torque is made up of rolling friction, dynamic friction and lubricant friction. [18]

$$M_{fric} = M_E + M_{RN}$$

$$M_{fri} = f_s \cdot WR \cdot DL2 + k \cdot \mu \cdot fA \cdot 0.95 \cdot e(0.15 \times nGWL) \cdot (M_{xy} + fL \cdot FR \cdot DL2 + FA \cdot DLk)$$

f_s : Bolt connection factor = 1.05

WR : Specific friction force [kN/m] = 1.53

DL : Raceway diameter [m] = 3.2

k : K-factor = 1.17

fA : Adjacent construction factor = 1

$nGWL$: Speed of the large diameter bearing. (*neglected*)

fL : Raceway factor fL = 1.73 (constant)

μ : Friction coefficient = 0.0015

FA : Axial load [kN] = 650

FR : Radial load [kN] = 730

Bending moment [kNm] = 30000

* M_{xy} , FA , FR are obtained from section 3

So, we have:

$$M_{fric} \cong 1.05 \times 1.53 \times 3.2^2 + 1.17 \times 0.0015 \times 1 \times 0.95 \times e^{0.15} (30000 \times 10^3 + 1.73 \times 730 \times 10^3 \times 3.8/2 + 650 \times 10^3 \times 3.8/1.17) \cong 82 \text{ kNm}$$

Moment of Inertia and Pitch Torque Calculation

Inertia of the Blade

To estimate the rotational inertia of the blade about the pitch axis, the blade is approximated as a thin ring with its mass concentrated at an effective radius.

Estimated radius: $r = 1.5 \text{ m}$

Blade mass = 20000 Kg

The moment of Inertia of a ring rotating about its central axis is given by:

$$J_{\text{blade}} = m_{\text{blade}} \cdot r^2 = 20000 \cdot (1.5)^2 = 45,000 \text{ Kg/m}^2$$

Total Inertia reflected to the Motor

The total inertia seen by the pitch motor consists of the blade inertia and the motor inertia reflected through the transmission system. This can be expressed as

$$\begin{aligned} J_{\text{total}} &= J_{\text{blade}} + i_{\text{total}}^2 \cdot J_{\text{motor}} \\ J_{\text{total}} &= 45,000 + (3000)^2 \cdot 0.287 = 2,628,000 \text{ kg/m}^2 \end{aligned}$$

Where:

i_{total}^2 = Total gear ratio

J_{motor} = Motor rotor inertia

Pitch Angular Speed and Acceleration Torque

The desired pitch angular speed(φ) is assumed 2 deg/sec

Converting degrees per second to radians per second:

$$2 \text{ deg/sec} \times \pi / 180 \approx 0.033 \text{ rad/s}$$

The acceleration torque required to reach this angular speed is calculated using

$$M_{\text{acc}} = J_{\text{total}} \times \varphi$$

$$M_{\text{acc}} = 2,628,000 \text{ kg/m}^2 \times 0.033 = 91 \text{ kNm}$$

Combining all the acting wind torque (M_z), the friction torque of the pitch bearing (M_{fric}), and the torque obtained from blade inertia (J)

$$M = 543 \text{ KNm}$$

Pitch Bearing Geometry and Ring Gear Dimensions

The blade is connected to the pitch bearing through a circular bolt pattern. Based on the blade root interface, the bolt circle diameter (BCD) is taken as 3400 mm

To accommodate the pitch bearing and ring gear arrangement, the effective gear pitch diameter (GPD) is selected slightly larger than the bolt circle diameter to ensure sufficient clearance and structural integrity.

Accordingly, the gear pitch diameter is estimated as:

$$GPD = 3526\text{mm}$$

Ring Gear and Pinion Tooth Count

For the gear dimensioning, the relationship between pitch diameter and number of teeth is given by:

$$Z=D/m$$

where Z is the number of teeth, D is the pitch diameter, and m is the module.

Using the selected pitch diameter and module, the number of teeth on the ring gear is obtained as:

$$Z_{ring} = 200$$

The pinion gear is selected with:

$$Z_{pinion} = 18$$

Gear Ratio Determination

The gear ratio of the pitch drive is defined as the ratio between the number of teeth on the ring gear and the pinion:

$$i_{bearing} = \frac{Z_{ring}}{Z_{pinion}} = \frac{200}{18} = 14.28$$

Torque at Pinion Level

The total torque required at the blade pitch axis was previously calculated as:

$$M = 543 \text{ KNm}$$

The torque acting on the pinion is reduced by the bearing gear ratio and the efficiency of the ring–pinion mesh. The required pinion torque is therefore given by:

$$M_{pinion} = (M) / (i_{bearing} \times \eta_{ring})$$

Assuming a ring gear efficiency of $\eta_{ring} = 0.96$:

$$M_{pinion} = 543 / (14.28 \times 0.96) = 40 \text{ kNm}$$

Total Transmission Ratio and Motor-Side Torque

The pitch system includes an additional gearbox stage between the motor and the pinion. The total transmission ratio is defined as:

$$i_{\text{total}} = i_{\text{gearbox}} \cdot i_{\text{bearing}}$$

Based on the selected drivetrain configuration, the total transmission ratio is estimated as:

$$i_{\text{total}} \approx 3000$$

The motor-side torque requirement is then calculated by accounting for the total gear ratio and transmission efficiencies:

$$M_m = \frac{M}{i_{\text{total}} \cdot \eta_{\text{gear}} \cdot \eta_{\text{pinion}}}$$

Where:

Gearbox efficiency: $\eta_{\text{gear}} = 0.93$

Pinion efficiency: $\eta_{\text{pinion}} = 0.96$

Substituting the values:

$$M_m \approx 203 \text{ Nm}$$

Next, we investigated the available electric motors in the market to find a suitable one. We chose IE5 Synchronous AC reluctance motor from *ABB* with a frame size is 200M a nominal power 22KW and a nominal rotational speed ($6P$) = 1000 1/min. The nominal torque is $M_{\text{nominal}} = 210 \text{ NM}$ while the maximum rotational speed can reach 4500 1/min and the ratio between the overload and nominal torque is 1.5. [19]

4.2.3.3 Specification of Motor

Motor Type		Synchronous AC reluctance
Designation		M3BL200MLB4
IE Class		IE5
Motor Efficiency		95.2 %
Maximum Speed		4500 Rpm
Current		47 A
Torque		210 Nm
Weight		304 Kg
Manufacturer		ABB

Table 8 : Specification of Motor

IE5 synchronous reluctance motors, network voltage 400 V

Output, kw	Type designation	Product code	Speed at 100% of nominal power (M) (r/ min)	IE class acc. to IEC	Motor efficiency with VSD supply T _N = 100%, nN = 100%	Typical IE3 induction motor efficiency with VSD supply*	Max speed, nmax	Current, I _N A	Torque	Rotor inertia (J = 1/4GD ²)	Weight, (M) (kgm ²)	Tempera- ture rise class (M)	
22	M3BL200MLB 4	3GBL202422-•SC	1000	IE5	95.0	91.1	4500	47.0	210	1.5	0.287	304	B

4.2.3.4 CAD Model of Motor



Figure 13 : Motor CAD Model of Optimus Syria

In case of Maximum Brake torque by considering the gear ratios of the blade bearing, the gearbox, and the Loads we have:

$$M_{brake} = \frac{MzB}{ibearing \cdot igear} \times \eta_{bearing} \times \eta_{gear}$$

$$M_{brake} = \frac{370}{13.81 \times 217.2} \times 0.95 \times 0.93$$

$$M_{brake} = 108.9 \text{ Nm}$$

Regarding the selecting of the proper gearbox, the *ABB* motor with frame size 200M and mounting configuration *IM B5* is fully compatible with the Bonfiglioli 711T3R gearbox due to its adherence to *IEC* standardized flange dimensions.

4.2.3.5 CAD Model of Gearbox

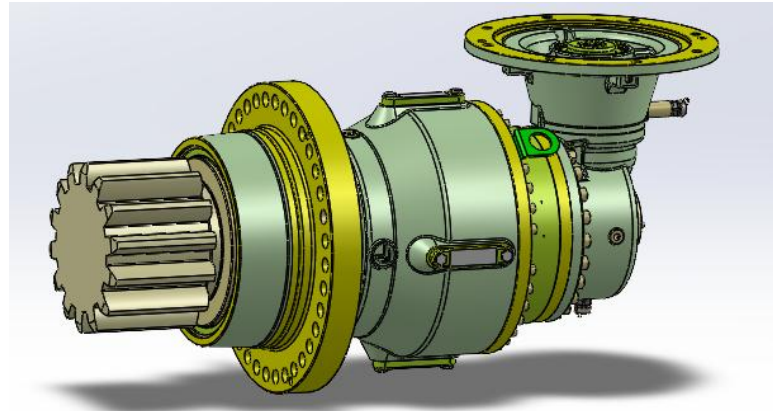


Figure 14 : Gearbox CAD Model of Optimus Syria

In terms of maximum torque, it will be implemented on the blade bearing's teeth:

$$M_{max, bearing} = 210 \times 1.5 \times 14.28 \times 217.2 = 977 \text{ kNm}$$

4.2.3.6 Specification of Pitch System

Pitch Drive Type	Electrical Pitch Drive (External Drive)
Gearbox	3 Stage Planetary Gearbox (Angular)
Motor Type	Synchronous AC Reluctance (22 KW)
Manufacturer	Bonfiglioli
Maximum Pitch rate	6° per second
Maximum Pitch Torque	977 KNm
Backup System	Battery
Total Gear Ratio	3000
Weight of the Pitch Drive	800 Kg
Pinion Module	18
Number of Teeth on Pinion	14

Table 9 : Specification of the Pitch System

4.2.3.7 CAD Model of Pitch Drive Assembly

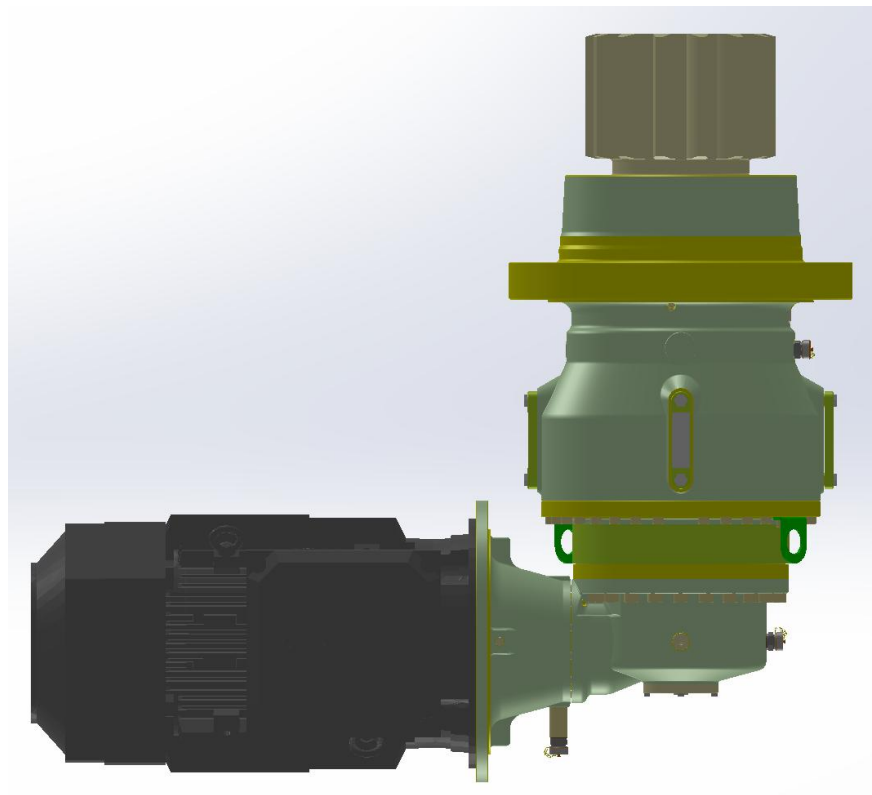


Figure 15 : Pitch Drive Assembly of Optimus Syria

4.2.3.8 Backup Supply System

Wind turbines operate in highly variable and sometimes extreme environmental conditions, where maintaining control and safety is essential. One of the most important systems in a turbine is the pitch control mechanism, which adjusts the blade angle to regulate power output and protect the turbine during high wind events or emergency situations. This system depends on a reliable source of power to respond quickly to changing conditions and to move the blades into a safe position when required. A dedicated backup power supply is therefore crucial, as it ensures uninterrupted operation even when the primary power source is unavailable. By providing stable energy during sudden load changes and emergency scenarios, the backup power system plays a key role in safeguarding turbine components, maintaining operational stability, and preventing potential damage, ultimately contributing to the overall reliability and longevity of wind turbines.[20]

Currently, backup power systems for wind turbine pitch mechanisms are often provided by lead-acid batteries or supercapacitors. Lead-acid batteries, however, have limitations such as a relatively short lifespan, low energy density, and environmental concerns. Supercapacitors offer high reliability and fast response but are often constrained by their high cost and limited energy storage capacity. In contrast, lithium-based batteries have become an increasingly attractive option for pitch system backup due to their well-developed technology, efficiency, and cost-effectiveness. Improvements in lithium battery technology, particularly in cathode

materials, have led to higher energy densities and better overall performance. Today, a variety of lithium battery chemistries are available, including lithium cobalt oxide, ternary compositions, lithium manganese oxide, lithium iron phosphate, and lithium titanate ($\text{Li}_4\text{Ti}_5\text{O}_{12}$), each offering distinct advantages for different operational requirements.[21]

There are two main options available in lithium batteries for wind turbine energy storage, but Lithium Iron Phosphate (LiFePO₄) is generally the superior choice over Lithium Titanate (LTO) for large-scale wind applications. While LTO is known for its extreme longevity, LiFePO₄ offers a much higher energy density (90 – 160 Wh/Kg) which is critical for storing the massive, intermittent surges of power generated during high-wind events without requiring an excessively large physical footprint. Furthermore, LiFePO₄ is significantly more cost-effective, often costing less per kilowatt-hour than LTO, making the high-capacity banks required for wind farms financially viable. Its chemical stability ensures high safety against thermal runaway, and with a cycle life that easily exceeds 3,000 to 6,000 cycles, it provides a reliable 10 to 15-year service life that aligns perfectly with the operational lifespan of most turbine hardware.[20]

a) Design and Sizing

In this study it used Lithium batteries as for its advantages mentioned above. The following steps summarize the sizing for batteries back-up system.

Assumptions & Estimations:

- ✓ The calculations focus on Single Axis Calculations: calculations for one axis and could be scaled appropriately if needed.
- ✓ Emergency Stop: The emergency stop system should allow for a single full cycle of pitching from 0° to 90° to ensure safety and functionality.
- ✓ Cycle 1: Emergency stop, pitching the blade from 0° to 90°.
- ✓ Cycle 2: Repositioning the blade back to 0° for safety or maintenance.

Energy Required for the motor side

From the 3 phase Ac electrical formula

$$E = \sqrt{3} \cdot U_N \cdot I_{\max} \cdot t \cdot PF$$

Where,

U_N : Nominal motor voltage (V)

I_{\max} : Maximum motor current (I)

PF: Power Factor

t : Time based on pitch rate (4°/s) = [180 (deg) / 4 (deg/sec)] · 2 = 90 sec

From our Motor specifications

U N: Nominal motor voltage (V) = 400

I max: Maximum motor current (A) = 47 A

PF: Power Factor = 0.85

t : Time based on pitch rate ($4^\circ/\text{s}$) = $[180 \text{ (deg)} / 4 \text{ (deg/sec)}] \cdot 2 = 90 \text{ sec}$

$$E = 2490.96 \cdot 24 \text{ J}$$

We divide by 3600 to convert Joules (J) into Watt-hours (Wh)

$$E = 691.93 \text{ Wh}$$

30% safety margin were added because the calculated energy is ideal. In reality, battery aging, temperature, inverter losses, and emergency loads require extra energy.

$$E = 691.93 \times (1+30/100)$$

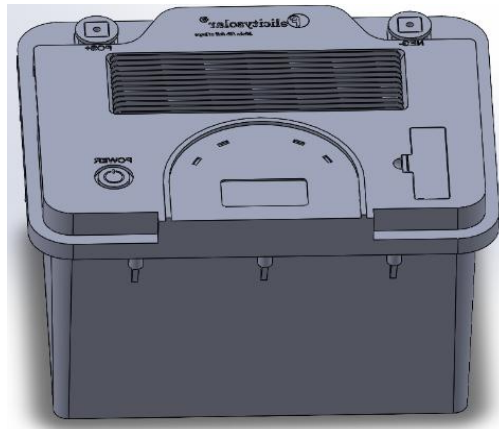
$$E = 900 \text{ Wh}$$

In Syria, calculating the energy for 5 emergency pitch cycles is a critical safety requirement for any wind turbine project. Due to the high risk of grid instability and frequent power outages in the region, the turbine must be able to perform a Safety feathering turning the blades out of the wind multiple times without relying on external power.

$$E = 5 \times 900 = 4500 \text{ Wh}$$

b) Battery selection

The Lion Tron LiFePO4 LX48-100 is chosen for the backup supply. It is a modular, high-performance battery storage system designed to meet the most demanding industrial requirements, making it an ideal choice for a wind turbine pitch system in Syria. This specific model provides a substantial capacity of 5120 Wh at a rated voltage of 51.2 V which is more than enough to handle the calculated requirement of 4500 Wh for emergency feathering. Its lithium iron phosphate (LiFePO4) chemistry is uniquely suited for the Syrian climate because it offers exceptional thermal stability, safely operating at discharge temperatures up to 60°C and storage temperatures as high as 65°C. Unlike other lithium types, this battery is designed with a high-quality integrated Battery Management System (BMS) that monitors for over-temperature and shuts down the system at 70°C to prevent damage. Furthermore, it is built for extreme durability with a cycle life of more than 6000\$ cycles at 90% depth of discharge, ensuring it can last the entire operational lifespan of the turbine without the frequent replacements required by lead-acid alternatives.

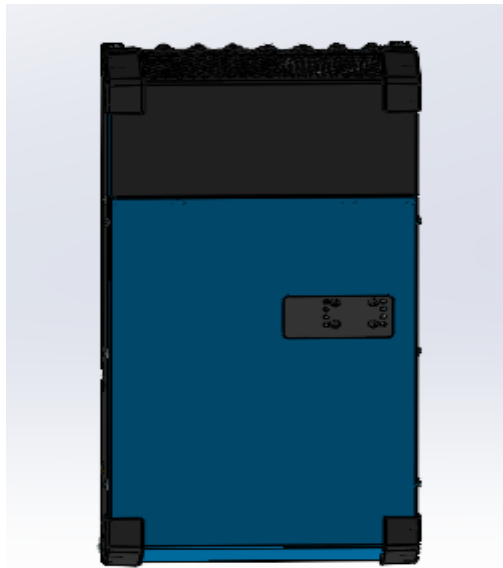
CAD Model of Battery*Figure 16 : Battery CAD Model of Optimus Syria*

Category	Specification
Rated capacity	100 Ah / 5120 Wh
Voltage range	43.2 V – 58.4 V
Weight	43.8 Kg
Dimensions (L × W × H) in mm	618 × 430 × 133
Battery Management System	Integrated
Certification	CE, RoHS, UN 38.3, MSDS

*Table 10 : Specification of Battery [22]***C) Inverter Selection**

The Victron MultiPlus-II 48V 3000VA inverter is chosen and it is well-suited for use with the selected battery system because its electrical characteristics closely align with the battery's specifications. The inverter's input voltage range is compatible with the battery's nominal voltage, allowing stable and efficient power conversion without additional voltage conditioning. It also supports configurable battery settings and includes a dedicated charging profile for lithium iron phosphate (LiFePO₄) batteries, ensuring proper charging behaviour, safety, and long battery life. The inverter's built-in charger operates within a current range that is well matched to the battery's capacity, enabling safe and effective charging without overstressing the battery. In addition, the system is designed to operate with a 48 V battery bank and reliably supply AC power to connected loads or serve as a backup power source, making it a compatible and reliable choice for the overall energy system.

Category	Specification
DC Battery Voltage (Nominal)	48 V DC
DC Input Voltage Range	approx. 38 – 66 V DC
Peak / Surge Power	approx. 5500 W
AC Output Voltage	120 V AC $\pm 2\%$
AC Output Frequency	60 Hz $\pm 0.1\%$
Operating Temperature Range	approx. 95 %
Maximum Efficiency	-40 °C to +65 °C

*Table 11 : Specification of Inverter [23]***CAD Model of Inverter***Figure 17 : Inverter CAD Model of Optimus Syria***4.4 Blade bearing**

For blade pitching to be implemented, it is essential to enable the rotor blades to rotate around their longitudinal axis. This rotational capability is essential for adjusting the blade's pitch angle, which optimizes energy capture and protects the turbine under various wind conditions. Although the required rotation angles and speeds are relatively modest, the blades are predominantly supported by bearings at their roots. [4]

Blade bearings connect to the rotor blade and the rotor hub of a wind turbine by means of bolted connections. Their rings tend to be made of steel, with 42CrMo4 type steel is the most common choice of material, whereas rolling elements are made from 100Cr6.[24]

4.4.1 Types of Bearings

The following basic design types are in commercial use as pitch and yaw rolling bearings of wind turbines:

a) Four-point contact ball bearings

Four-point contact ball bearings are the most commonly used bearing type in wind turbine pitch systems. In smaller turbines, they are typically designed with a single row of balls, while larger turbines usually employ a double-row configuration. These bearings can support loads in all directions and are capable of accommodating relatively large deformations at the interface, which makes them suitable for pitch applications. Double-row four-point contact ball bearings rely on point contact between the balls and raceways, resulting in high contact stresses. With an initial contact angle of 45 degrees, they can withstand combined axial and radial loads. However, their load-carrying capability is lower compared to triple-row roller bearings due to the smaller contact area. Under heavy loading conditions, these bearings are susceptible to significant ring deformation and potential ring separation, which can reduce service life. They are also prone to edge loading, as the balls tend to shift toward the raceway edges when loaded, increasing localized stress and wear. Moreover, while they can handle substantial radial loads, the resulting cyclic stresses in the bearing rings may lead to fatigue over prolonged operation.

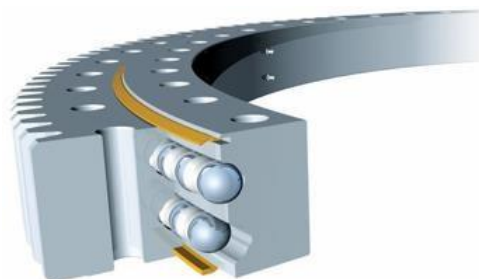


Figure 18 : Double row four-point contact ball bearing external toothed [25]

Despite certain limitations, this type of bearing provides several notable advantages. Both raceways share the applied load at the same time, which improves load distribution and enhances overall stability. Their design is relatively simple compared to triple-row roller bearings, resulting in moderate manufacturing complexity. As a result, production costs are lower, making these bearings a cost-effective solution for applications where economic considerations are important. The point contact between the rolling elements and raceways also helps reduce friction and surface wear. However, when exposed to very high loads, their service life is reduced, which restricts their suitability for more demanding or extreme operating conditions.[26]

b) Three-row roller bearings

The three-row roller bearing has two rows of axial roller elements that help it endure axial loads and one row of radial roller elements that help it survive radial loads. These two-row roller components aid in absorbing heavy radial loads.



Figure 19 : Three raw rollers bearing with internal toothing [25]

Triple-row roller bearings feature a line contact design, which results in lower contact pressure compared to other bearing types. Their contact angle arrangement—90 degrees for the axial rows and 0 degrees for the radial row—allows them to efficiently support both axial and radial loads. The large contact area provides a very high load-carrying capacity, making these bearings suitable for applications that require strong and reliable performance. They exhibit minimal bearing ring deformation and very low risk of ring separation under heavy loads, which significantly improves their durability. Edge loading caused by roller tilting during deformation is generally limited, and radial loads are handled effectively with low stress levels due to the presence of a dedicated radial roller row.

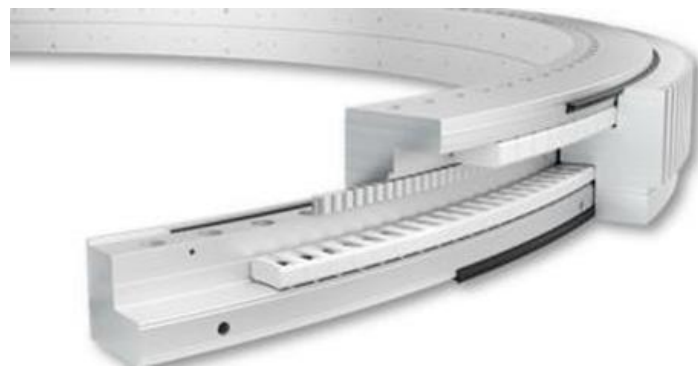


Figure 20 : Three raw rollers bearing with External toothing,2024 [25]

However, the complex structure of triple-row roller bearings leads to high manufacturing complexity and, consequently, higher production costs. Despite this, their robust construction ensures a long service life, making them ideal for applications where long-term reliability and durability are critical. In addition, for the same load capacity, these bearings are more compact than double-row four-point

contact ball bearings, which makes them particularly suitable for applications such as the Optimus Syria wind turbine.

c) Three-row ball and roller bearings

This type of bearing is an improvement of double row four-point contact ball bearing. Three row ball and roller bearings tend to have lower radial deformations under load than four-point contact ball bearings, but they do not provide significantly higher load ratings. This is why this type of bearing is not used in large-capacity wind turbine.

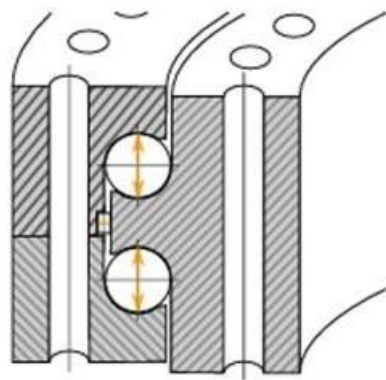


Figure 21 : Three raw ball and roller bearing [27]

4.4.2 Blade attachment

The connection of Wind turbine blades with the hub can be possible via two different concepts, inner rotating and outer ring rotating. Each choice has its own advantages and disadvantages. Many aspects influence the decision, such as the cost of the surrounding parts, assembly processes, Maintenance accessibility and technical feasibility, this is a very important step, which will again influence the further design of the Hub.

4.4.2.1 Comparison of Inner Ring and Outer Ring Rotating Configurations

Pitch bearing configurations can be broadly classified into inner ring rotating and outer ring rotating designs, each offering distinct advantages. In the inner ring rotating configuration, the blade is mounted on the inner ring while the outer ring is fixed to the hub. This arrangement provides high structural stiffness, allows the use of stiffener plates, and improves load distribution due to the larger effective diameter.



Figure 22 : Inner Ring mounted blade, 2024 [8]

In contrast, the outer ring rotating configuration, where the blade is attached to the outer ring and the inner ring is fixed to the hub, offers several advantages that make it more suitable for the Optimus Syria turbine. This design enables a more compact and lightweight hub, reducing overall structural mass and simplifying the hub design. It also creates additional space inside the hub, which improves the layout of internal components and facilitates cable routing and lubrication system integration. From a manufacturing and installation standpoint, the outer ring configuration is more economical and easier to assemble, which is particularly beneficial for turbines intended for cost-sensitive and logistically challenging environments.



Figure 23 : Outer Ring mounted blade, 2024 [28]

While the inner ring configuration emphasizes stiffness and safety, the outer ring rotating design provides superior benefits in terms of compactness, weight reduction, spatial efficiency, and overall system simplicity. With appropriate protective measures and robust design practices, the operational

risks can be effectively managed. Therefore, considering the design priorities of the Optimus Syria turbine, the outer ring rotating configuration represents the more advantageous and practical solution.

4.4.3 Dimensioning of the Three-row roller bearing

The statical calculations aim to ensure that the blade bearing can withstand the maximum load situations occurring for all operating conditions of the turbine.

The calculation starts with the analysis of the load time series for the DLCs in order to identify the maximum resulting bending moment.

The dominant load of a pitch bearing is the resulting moment (M_{xy}) Which is the combination of flap-wise and edgewise bending moment.

$$M_{xy} = \sqrt{M_x^2 + M_y^2}$$

Radial (F_z) and Axial (F_{xy}) forces influence the rolling body loads as well

The following loads taken for the calculation (cf. Section 3-Loads)

Bending Moment $M_{xy} = 30000 \text{ kN/m}$

Radial force (F_z) = 650 kN

Axial force (F_{xy}) = 730 kN

Assumption for the Calculations:

The upper and lower axial raceways have the same raceway diameter D_{pw} , [mm]

The upper and lower axial raceways have the same roller diameter D_w [mm]

Roller length L [mm] = roller diameter D [mm]

The radial raceway is not considered

Calculation of Hertzian pressure

For the calculation of the Hertzian pressure we followed procedure as given by our supervisor.

- Define raceway system parameters (D_{pw} , D_w , L and Z)

Set raceway diameter D_{pw} [mm]

For calculating D_{pw} (bearing raceway diameter), bolt circle diameter D_{bcd} need to consider. Which was 3400 mm , given by the Blade team.

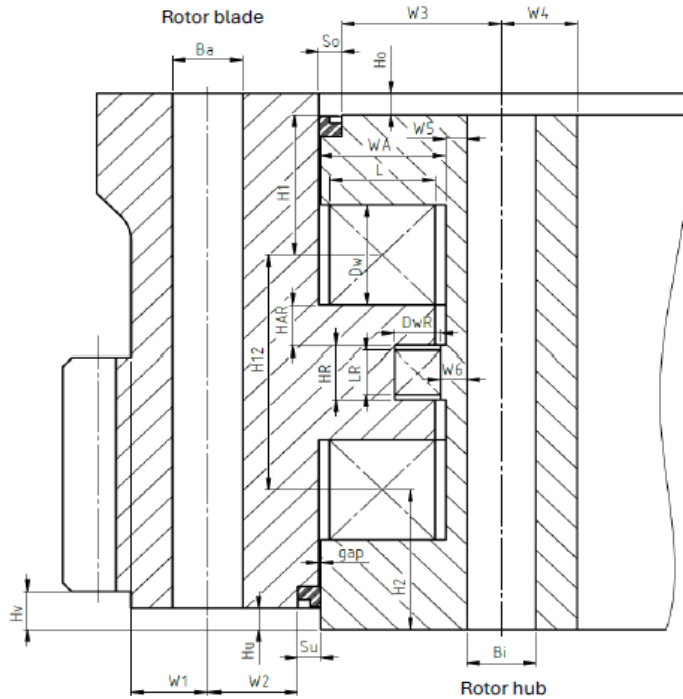
Pitch bearing with external teeth

Figure 24 : 2 D Sketch of Three-row roller bearing (External teeth)

Set roller diameter Dw [mm]

Roller diameters up to 80 mm would theoretically be possible (from raceway surface hardening point of view). However, the length of the rollers can cause large bearing ring deformations. Therefore, roller diameters greater than 65 mm should be avoided.

Use roller diameters 50, 55, 60, 65 mm.

$$Dw = 60 \text{ mm}$$

$$\text{Roller length } L \text{ [mm]} = \text{roller diameter } Dw \text{ [mm]} = 60 \text{ mm}$$

Estimate number of rollers per axial raceway Z for the given Dpw and Dw :

$$Z = \pi * Dpw / Dw * 1.15 = 145$$

Calculate maximum roller force (Q_{\max})

Maximum roller force for ideal conditions (rigid companion structure, same stiffness over the entire bearing circumference): [36]

$$Q_{\max_rigid} = F_z/Z + 4.1 \cdot M_{xy}/D_{pw} \cdot Z = 269.5 \text{ kN}$$

The influence of the companion structure can be considered by an additional factor K_q : and For good rotor blade and rotor hub designs: $K_q \leq 1.15$.

$$Q_{\max_flexible} = K_q \cdot Q_{\max_rigid} = 309.92 \text{ kN}$$

The highest contact force Q_{\max} obtained which is used to calculate the highest resulting Hertzian pressure p_{\max} .

Calculate maximum contact stress (p_0)

The Hertzian calculations cannot be solved analytically. Hence, equations for an approximation were well established. For example, Houpert published a method. The maximum pressure (p_{\max}) follows according to 3.3, the Hertzian contact ellipse radii are required inputs for the equation. Here, another iterative process comes into play

$$b = 0.00335 * \sqrt{Q_{\max_flexible} L_{we}} * \Sigma \rho = 1.37$$

$$L_{we} = L - (2 * r_{\text{axial}}) = 61 \text{ mm}$$

$$p_{0\max} = 2 * Q_{\max_flexible} / \pi * b * L_{we} = 2453.32 \text{ N/mm}^2$$

Due to bearing ring deformation, the rollers tilt leading to an uneven pressure distribution and thus higher contact stresses. This can be considered by an additional factor K_p : For stiff bearing design, $K_p \leq 1.20$. [36]

$$p_{\max} = p_{0\max} * K_p (1.20) = 2943.99 \text{ N/mm}^2$$

According to ISO 76, Permissible contact stresses shall be less than 4.2 GPa for ball bearings and 4.0 GPa for roller bearings. However, since these pressures are related to extreme wind conditions, typical contact pressures during normal operation of the turbine are lower. However, when using the criterion 3300 N/mm², it is likely that the bearing is also feasible for the fatigue loads.

4.4.4 Pitch Bearing Safety Factor Calculation

The load limit for gear wheels is determined by the load capacity. According to DIN 3979, there are three main types of damage to gears that determine the load limit

- Tooth breakage due to excessive bending stress in the tooth root,
- Tooth flank fatigue due to material fatigue (pitting, chipping),
- Scuffing due to the combined effect of pressure and sliding speed.

Tooth breakage typically refers to the complete or partial fracture of a tooth when its load-bearing capacity is surpassed. To prevent this, the safety and integrity of the tooth root must be evaluated.

Fatigue on tooth flanks appears as pitting when the contact pressure exceeds the tolerable limit. Repeated loading and unloading cause material fatigue, leading to pits after numerous rollovers. This is critical only if pitting worsens with service life or pits grow larger, indicating diminished load capacity due to exceeded permissible flank pressure, so the load capacity of the tooth flank needs to be checked.

Maximum forces,

By given Maximum torque of 977 kNm, the tangential force on the gear teeth can be calculated, as follows: [29]

$$F_{t,12} = 2*T_{max}/d_2 = 537.4 \text{ kN}$$

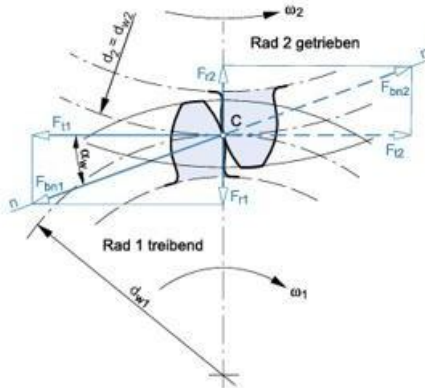


Figure 25 : Forces on Gear[29]

where,

d_2 = effective diameter of pitch bearing gear teeth,

$$Mn^*Z_2 = 3440 \text{ mm},$$

This Tangential force is divided into two components as shown in fig, the normal tooth force F_b (perpendicular to the flank and mating flank at the point of contact) and the radial force (always directed towards the respective wheel centre) F_r .

Since α is the same as (20°) these forces can be calculated with the following equations: [29]

Normal tooth force [29]

$$F_{bn12} = F_{t1,2}/\cos\alpha = 571.8 \text{ kN}$$

Radial force [29]

$$F_{rn12} = F_{t1,2} * \tan\alpha = 195.6 \text{ kN}$$

Nominal forces:

With the given nominal torque of 250 kNm per pitch system the tangential force on the gear can be calculated by the following equation. [29]

$$F_{t,12_nomi} = 2 * T_{nomi} / d_2 = 149.33 \text{ kN}$$

Stress Influencing Factors

For practical design, simplified methods (C & D) are often used as most industrial gearboxes operate in the subcritical range, ensuring faster calculations with sufficient accuracy.

The application factor (operating factor) K_a , accounts for external additional forces specific to the input and output machines connected to the gearbox. These forces include shocks, torque fluctuations, and load peaks. [29]

$$K_a = 1$$

Dynamic factor K_v , it records the internal dynamic additional forces that arise under load due to deformation of the teeth wheel centre and all other force-transmitting elements of the gearbox. [29]

$$K_v = 1 + (K_1 / F_{t,12_nomi} * K_a + K_2) * K_3 = 1$$

Where,

$K_1 = 24.5$; Gear quality 8 considered

$K_2 = 0.0193$

$$K_3 = 0.01 * Z_1 * V_t * \sqrt{(u^2) / (1 + u^2)} = 0.00617$$

Face Width Factors

Face width factors " $K_{H\beta}$ " and " $K_{F\beta}$ ". They take into account the effects of uneven force distribution over the tooth width on the flank stress (' $K_{H\beta}$ ') or on the tooth root stress (' $K_{F\beta}$ '). This is caused by the flank line deviations that occur in the loaded state as a result of mounting and elastic deformations (F_{sh}) and manufacturing deviations (F_{ma}).

$$K_{H\beta} = 1 + 10 * F_{\delta y}(F_{tnomib}) = 1.2$$

Taking into account the following influencing variables:

F_{sh}) Flank line deviation due to deformation can be determined as a first approximation from experience. [29]

$$F_{sh} = 0.023 * (F_{tnomib}) * [0.7 + K' * (l * sd12) * (d1dsh)4/3] * (bd1)^2 = 5.42 \mu m$$

Where,

d_1 = pitch circle diameter of pinion = 256 mm

b = tooth width = 162.5 mm

$$(F_{tnomib}) = Kv * (Ka * F_t / b) = 1456 \text{ N/mm}$$

Now, we have to find F_{ma} . It is production-related flank line deviation as below,

$$F_{ma} = c * 4.16 * b * 0.14 * q_H = 20.6012 \mu m$$

Where,

$c = 1$ for wheel pairs without adjustment measures

$$q_H = 2.59,$$

Effective flank line deviation before running-in [29]

$$F_{\beta X} = F_{ma} + 1.33 * F_{sh} = 27.80 \mu m \quad (4.42)$$

This amount is reduced by the run-in amount ‘y’ according to TB 21-17, so that after the run-in the effective flank line deviation is [29]

$$F_{\beta Y} = F_{\beta X} - yb = 21.80 \mu m$$

Where,

$$yb = 6$$

The exponent for determining the width factor for the tooth root results from [29]

$$Nf = (b/h)^2 / [1 + (bh) + (bh)^2] = 0.644$$

When this is done, the tooth base width factor is calculated [29]

$$KF\beta = KH^6 Nf = 1.18$$

Next values for the face load factor $KH\alpha$ and $KF\alpha$ are assumed according to [29], with the tooth quality of 8 and regular straight gears [29]

$$KH\alpha = KF\alpha = 1.1$$

With all these values the total influence factors $KFges$ (tooth base strength factor) and

$KHges$ (tooth flank/pitting factor) are determined [29]

$$KFges = Ka * Kv * KFa * KF\beta = 1.29$$

$$KHges = \sqrt{Ka * Kv * Kha * Kh\delta} = 1.23$$

The maximum local tooth root stress occurring when a fault-free gear is loaded by the static nominal torque can be determined from

$$\sigma_{f01} = F_{t12nomi} / b * mn * Y_{fa} * Y_{sa} * Y_{\varepsilon} = 166.26 \text{ N/mm}^2$$

Where,

$Y_{fa} = 2.42$ (Form factor)

$Y_{sa} = 1.82$ (Stress correction factor)

$Y_{\varepsilon} = 0.25 + 0.75\varepsilon\alpha = 0.6667$ (Overlap Factor)

Total tooth root stress can be calculated as follows,

$$\sigma_{f12} = \sigma_{f01} * KFges = 223.50 \text{ N/mm}^2$$

Tooth root limit strength can be calculated by

$$\sigma_{fg1} = 2 * \sigma_{flim} * Y_{NT} * Y_X = 642 \text{ N/mm}^2$$

Where,

$\sigma_{flim} = 369 \text{ N/mm}^2$ for Bearing and 500 N/mm^2 for the Pinion

$Y_{NT} = 1$ (Service life factor)

$Y_X = 0.87$ (Size Factor)

Safety of the tooth root load capacity

$$Sfl = \sigma_{fg1} / \sigma_{f1} = 2.07$$

Verification of pit load-bearing capacity

The calculation of the pitting load-bearing capacity is based on the flank pressure σ_H at the rolling point, and the flank pressure that occurs at the rolling point is [29]

$$\sigma_{H0} = ZH * ZE * Z\varepsilon * Z\delta * \sqrt{(u+11)} (F1b * d1) = 946.70 \text{ N/mm}^2$$

Where,

Z_H is zone factor, takes into account the flank curvature at the rolling point, which is

2.5 for straight gears

Z_E is Elasticity factor, which is 189.8 N/mm^2

Z_S is Coverage factor, takes into account the influence of the load distribution on several pairs of flanks involved in the engagement on the calculated Hertzian pressure, which is 0.825

Z_W is Screw factor, it records the improvement in load-bearing capacity under flank pressure with increasing helix angle, which is 1.

Flank pressure occurring at the rolling circuit is

$$\sigma_H = \sigma_{H0} * K_H g_e s = 1164.45 \text{ N/mm}^2$$

Flank Limit Strength

Flank limit strength can be determined by the following equation [29]

$$\sigma_{HG} = \sigma_{Hlim} * Z_{NT} * Z_L * Z_V * Z_R * Z_W * Z_X = 1743.22 \text{ N/mm}^2$$

Where,

σ_{Hlim} is tooth flank fatigue strength, 1204.44 N/mm^2

Z_{NT} is Service life factor, takes into account a higher permissible pressure if a limited-service life is required in timing gears, which is 1.

Z_L is Lubricant factor, for mineral oils depending on the nominal viscosity at 50° or 40° , which is 1.

Z_V is Velocity factor, takes into account the influence of the circumferential speed on the flank load-bearing capacity, which is 0.89

Z_R is Roughness factor, determines the influence of surface roughness, which is 0.87

Z_W is Material pairing factor, takes into account the increase in flank strength of a gear made of structural steel, heat-treated steel, which is 1.

Z_X is Size factor, calculates the influence of the tooth dimensions, which is 0.87

Safety of the Flank Load Capacity

$$SH12 = \sigma_{HG} / \sigma_H = 1.49$$

4.4.5 CAD Model of Bearing and its Dimensions

Bearing Type	Triple row roller bearing
Inner BCD of Bearing	2994 mm
Outer BCD of Bearing	3400 mm
Bolts on inner BCD	125 × (M36)
Bolts on outer BCD	142 × M36)
Gear Module	18 mm
Pitch Circle Diameter	3600 mm
Number of teeth	200
Material	42crM04
Weight	8T
Height	328 mm
Outer Diameter	3636 mm

Table 12 : Specification of Bearing



Figure 26 : Bearing CAD Model of Optimus Syria

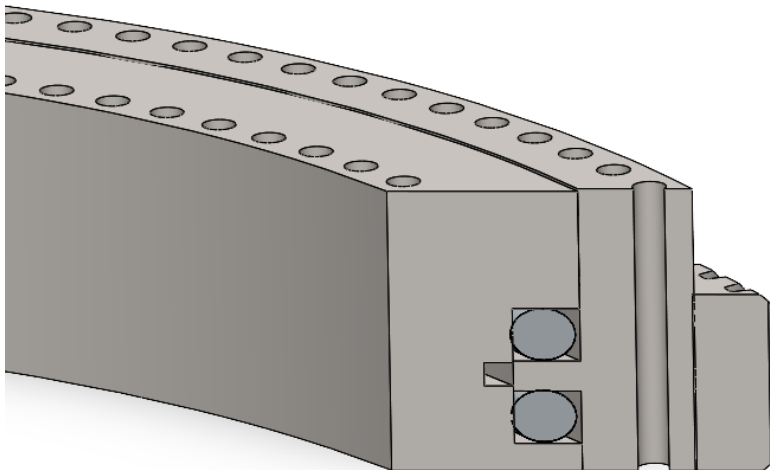


Figure 27: Cross-section view of Bearing

4.5 Lubrication System

The lubrication system is a critical component for the reliable operation of pitch bearings in wind turbines. Pitch bearings operate under demanding conditions, characterized by high loads, oscillating motion, low rotational speeds, and exposure to harsh environmental factors such as dust, moisture, temperature extremes, and wind-driven contaminants. Under these conditions, effective lubrication is essential to reduce friction between rolling elements and raceways, minimize wear, and prevent surface damage such as fretting, pitting, and corrosion.

A properly designed lubrication system ensures that an adequate and consistent lubricant film is maintained across all contact surfaces within the pitch bearing. This film reduces metal-to-metal contact, lowers contact stresses, and helps distribute loads more evenly among the rolling elements. In addition, lubrication plays a vital role in dissipating heat generated during operation and in protecting the bearing surfaces from environmental contamination. For pitch systems, where movements are often small and intermittent rather than continuous, lubrication is especially important to prevent lubricant starvation and uneven grease distribution.

The lubrication system also has a direct impact on the service life and maintenance requirements of the pitch bearing. Reliable lubrication reduces the likelihood of premature bearing failures, which can lead to costly downtime, difficult repairs, and safety risks. In wind turbines, where pitch bearings are large and difficult to replace, maintaining optimal lubrication is far more economical than corrective maintenance. For the Optimus Syria turbine, an effective lubrication strategy supports long-term durability, operational safety, and consistent pitch system performance, making it a key factor in ensuring overall turbine reliability.[30]

4.5.1 Comparison of Manual and Automatic Lubrication

Feature	Manual Lubrication	Automatic Lubrication
Lubrication Frequency	Periodic (scheduled stops)	Continuous intervals
Accuracy of Grease dosage	Low -operator dependent	High controlled & consistent
Downtime	Requires stopping turbine	Can operate while running
Reliability	Medium	Very high
Cost	Low initial cost	Higher initial cost

Table 13 : Comparison of Manual and Automatic Lubrication[30]

Automatic lubrication is chosen over manual lubrication because it provides a more reliable, consistent, and efficient solution for demanding wind turbine operating conditions. Manual lubrication depends heavily on maintenance intervals and human accuracy, which can lead to uneven grease distribution, missed lubrication cycles, or over-lubrication. In contrast, automatic systems supply controlled amounts of lubricant at regular intervals, ensuring continuous protection of the bearing during operation. This is especially critical for pitch bearings, which experience high loads and slow, oscillating motion. By reducing maintenance effort, minimizing human error, and ensuring optimal lubrication at all times, automatic lubrication significantly improves bearing reliability, extends service life, and enhances the overall safety and availability of the wind turbine.

4.5.2 Types of Automatic Lubrication Systems

Type	How it works	Advantages	Limitations
Progressive Distributor System	One pump → primary metering block → secondary blocks → grease flow through a fixed sequence	High reliability, blockage detection, equal distribution, good for large bearings	The entire system stops if one outlet blocks (but gives alarm)
Injector system	Each injector delivers a metered shot independently	Can supply different outputs per point	Injectors require pressure reset cycles; more complex to maintain

Table 14 : Comparison of Automatic Lubrication Systems [30]

Progressive lubrication systems are preferred because they offer the most reliable and controlled grease delivery. Each lubrication point receives a precisely metered amount of grease in a fixed sequence, ensuring uniform distribution across all bearing rows. Blockages are immediately detected because the metering pistons stop in sequence, allowing early fault identification and preventing bearing damage.

4.5.3 Grease volume calculation

The amount of grease required is determined by calculating the free internal space available inside the bearing that can be filled with grease. A roller bearing consists of three raceways, rollers, and a cage. The raceways provide the annular space, but this space is not fully empty—rollers and cage occupy part of the volume. Therefore, the grease volume is calculated by:

$$\text{Amount of Grease Required} = \text{Volume of 3 Raceway} - (\text{Volume of Roller} \times \text{Number of Rollers})$$

Parameters:

Raceway outer diameter $D_o = 3229 \text{ mm} = 3.229 \text{ m}$

Raceway inner diameter $D_i = 3169 \text{ mm} = 3.169 \text{ m}$

Width $B = 61.5 \text{ mm} = 0.0615 \text{ m}$

Roller diameter = 60 mm → radius = 30 mm

Roller length assumed = 60 mm

Number of rollers = 145

Grease density = 0.90 kg/L

Fill fraction = 80%

Relubrication fraction = 50% per year

Raceway volume (one row)

$$V = \pi (R_o^2 - R_i^2)B$$

$$R_o = 1.6145, R_i = 1.5845 \text{ m}$$

$$R_o^2 - R_i^2 = 0.0955 \text{ m}^2$$

$$V = \pi \times 0.0955 \times 0.0615 = 0.01854 \text{ m}^3 = 18.54 \text{ L}$$

For Three Raceway

$$V_{\text{raceway, total}} = 3 \times 18.54 = 55.62 \text{ L}$$

Subtract roller volume

$$\text{Volume occupied by rollers} = V_{\text{roller}} \times N_{\text{rollers}} = 24.59 \text{ L}$$

$$V_{\text{grease}} = 55.62 - 24.59 = 31.03 \text{ L}$$

Subtract cage pocket volume (15% of remaining space)

$$V_{\text{grease usable}} = 31.03 \times (1 - 0.15) = 31.03 \times 0.85 = 26.375 \text{ L}$$

Convert grease volume (liters) into mass (kg) because grease is purchased, applied, measured, and calculated in mass, and density differences make mass the only reliable engineering unit.

$$M_{\text{filled}} = V_{\text{grease usable}} \times \rho \times \text{fill fraction}$$

$$M_{\text{filled}} = 26.375 \times 0.90 \times 0.80 = 18.99 \text{ kg}$$

Annual Re-Lubrication

Per manufacturer guidelines, 50% of filled mass is required annually:

$$M_{\text{annual relub}} = 18.99 \times 0.50 = 9.495 \text{ kg/year}$$

Additional pitch-bearing gear requires:

$$5.00 \text{ kg/year}$$

$$\text{Total annual requirement} = 9.495 + 5.00 = 14.495 \text{ kg/year}$$

Maintenance Interval Requirement

For a 6-month maintenance cycle:

$$\text{Monthly consumption} = 14.495 / 12 = 1.207 \text{ kg/month}$$

$$\text{Grease for 6 months per bearing} = 1.207 \times 6 = 7.24 \text{ kg}$$

For 3 identical bearings:

$$7.24 \times 3 = 21.72 \text{ kg per maintenance cycle}$$

4.5.4 Grease Type Selection

For wind turbine pitch bearings, the grease must:

- ✓ Handle oscillating motion / very small angular rotation
- ✓ Resist fretting corrosion
- ✓ Have wide temperature stability
- ✓ Allow long lubrication intervals
- ✓ Work with automatic lubrication systems

In this design, SKF LGWM 2 heavy-duty EP grease is selected. This grease is formulated for extreme pressure operation, includes a high-viscosity synthetic base oil and molybdenum additives to prevent

metal-to-metal contact under boundary lubrication, and retains stability over a wide temperature interval of -40°C to $+120^{\circ}\text{C}$, making it well adapted for both winter cold spells and summer desert conditions typical of Syrian onshore installations. SKF lubricants also carry OEM approvals from major turbine manufacturers, including Vestas, GE, and Nordex, thus ensuring compatibility with industry-standard progressive lubrication systems and long-interval maintenance cycles that reduce operational downtime.[31]



Figure 28 : SKF Grease [31]

4.5.5 Lubrication pump and Reservoir calculation

The lubrication system for the pitch bearings is designed based on the grease density of 0.9 kg/L to meet the relubrication requirements over a 6-month period.

Total Tank volume calculation

$$\text{Total Grease Volume} = (28.24 \text{ kg} / 0.9 \text{ Kg/L} = 24.1 \text{ L}) \approx 30 \text{ L}$$

To continuously deliver grease to the three pitch bearings, an automated SKF KFG 2 central lubrication pump is implemented. A 30 L tank is selected to avoid under-lubrication during periods of prolonged operation or delayed maintenance. The KFG2 system is designed for harsh industrial applications, supports up to three lubrication circuits, features automatic purge and refill control.

The selected grease provides strong fretting-corrosion resistance, maintains viscosity across a -40°C to $+120^{\circ}\text{C}$ temperature range, and is validated for use in OEM wind turbine lubrication systems. Its formulation, containing high-viscosity synthetic oils and molybdenum-based additives.

This pump-reservoir-grease combination ensures that continuous automated lubrication is maintained during turbine operation, improving bearing lifespan, reducing maintenance downtime and enhancing overall turbine availability. [32]



Figure 29 : Lubrication Pump [32]

Technical data of the pump

Parameter	Values
Maximum back pressure	12/24 VDC
Ambient temperature ¹⁾	300 bar
• with spring-return pump elements:	-25 °C to +70 °C
• with positively actuated pump elements:	-30 °C to +70 °C
Pump elements	Max. 3
Reservoir material	PMMA
Mounting position ²⁾	Vertical
Sound pressure level	< 70 dB (A)
Duty type/cycle as defined by IEC 60034-1, DIN EN 60031-1, and VDE 0530-1	S1 continuous operation
Nominal speed ³⁾	<ul style="list-style-type: none"> • 12 VDC: 15 rpm, ±2 rpm • 24 VDC: 17 rpm, ±3 rpm
Mechanical lubricant level switch	NLGI Grade 2
Type identification code 1 (W1)	Fault notification via pulse
Mechanical lubricant level switch with signal smoothing, type identification code 2 (W1G)	NLGI Grade 2
Electrically controlled pressure relief valve	Fault notification via energized contact
	12 VDC or 24 VDC, see Pressure relief valve with integrated pressure limiting valve,

4.5.6 Lubrication Pinion

A lubrication pinion is a specialised gear-shaped applicator that automatically transfers lubricant to the mating surfaces of open gears and racks. It is engineered to deliver grease or oil evenly across the tooth flanks as the pinion rotates in mesh with the gear, replacing manual brushing or spraying methods and ensuring consistent lubrication where gears meet.

Lubrication Pinon	
Material	Polyurethane (PU)
Number of Teeth	14
Module	18
Maximum admissible volume flow	2 l/m^2
Maximum Speed	80 rpm
Operating temperature	-30 to 70

Table 15 : Specification of Lubrication Pinion [33]

4.5.7 CAD Model of Lubrication Pinion

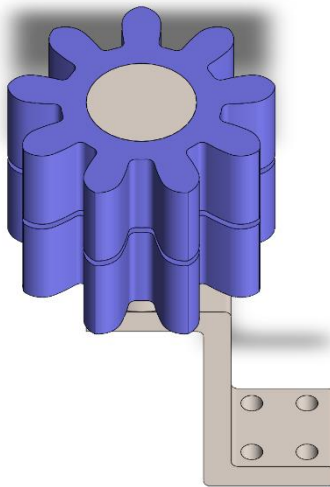


Figure 30 : Lubrication Pinion CAD Model of Optimus Syria

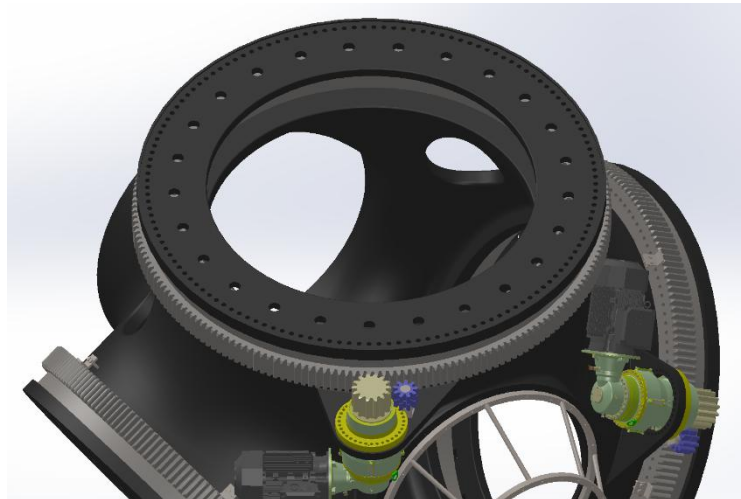


Figure 31 : Lubrication pinion engagement with blade bearing ring gear

4.6 Labyrinth Sealing

In a wind turbine, the rotor blades attach to the Hub (which is enclosed by the spinner). The junction between the blade and spinner must be sealed to prevent rainwater or moisture from entering the hub, which houses critical mechanical components like the pitch bearing and hydraulic or electrical systems.

Labyrinth Seal Design between Rotor Blade and Spinner. To prevent the ingress of rainwater from the rotor blade into the hub assembly, a labyrinth sealing system is implemented between the blade root and the spinner. This sealing arrangement ensures the protection of critical hub components, such as the pitch bearings and coupling interfaces, from moisture-induced degradation and corrosion. The proposed design incorporates a Glass Reinforced Plastic (GRP) ring attached around the blade surface near the root section. This GRP ring overlaps with a collar that forms an integral part of the spinner structure.

The interaction between these two geometries forms a non-contact labyrinth path that resists direct water entry while maintaining freedom for rotational or dynamic blade movements. Furthermore, the inner diameter of the GRP ring is designed to be sufficiently large to facilitate maintenance operations such as the removal or replacement of blade bearings without necessitating the complete disassembly of the spinner.

This design offers both functional sealing and service accessibility, which are essential for reliable and efficient turbine operation.

1. Function of the Labyrinth Seal: The main function of the labyrinth seal is to prevent water or moisture from entering the hub (the central part of the turbine that connects all blades).

2. Construction Concept: A ring made of GRP (Glass Reinforced Plastic) or a similar material can be glued to the blade root section. This GRP ring covers a collar that is part of the spinner (the nose-cover of the rotor hub assembly). Basically, the blade side has a GRP ring attached. The spinner side has a collar or lip that fits inside or outside that ring.

Together they form the labyrinth seal path—a small, complex gap that blocks direct entry of water.

3. Dimensional Consideration: The diameter of the sealing ring must be large enough to allow for blade bearing maintenance or replacement.

This means technicians should be able to remove the blade bearing through the opening created by the seal without dismantling the entire spinner structure.

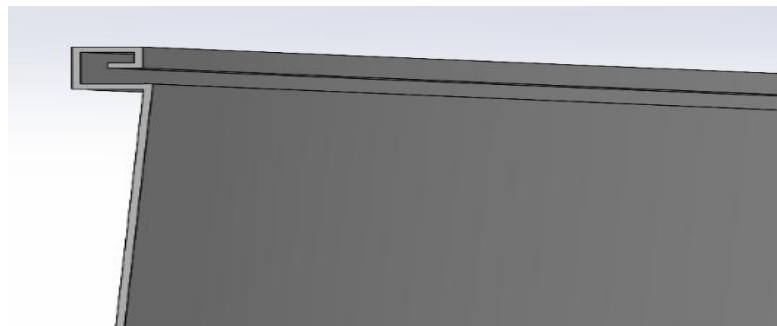


Figure 32 : Cross-section view of Lab Sealing of Blade

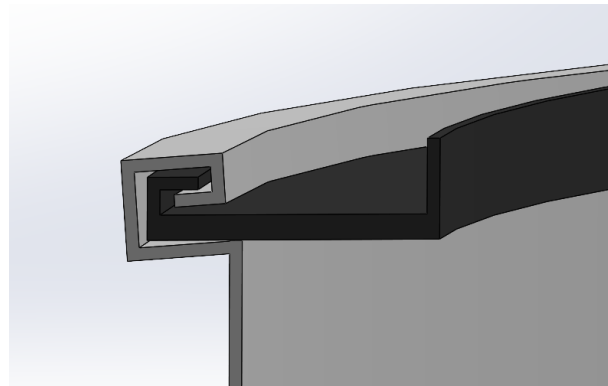


Figure 33 : Spinner Cross-section view Lab Sealing

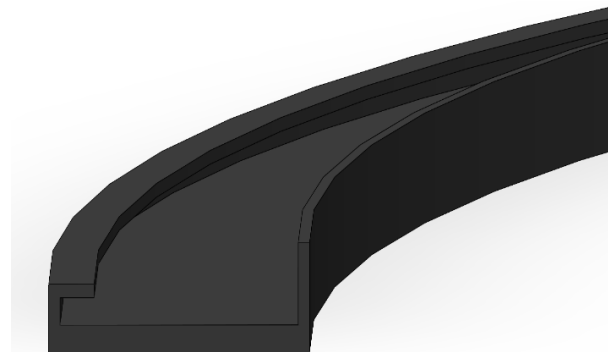


Figure 34 : Cross-section view Lab Sealing of Blade

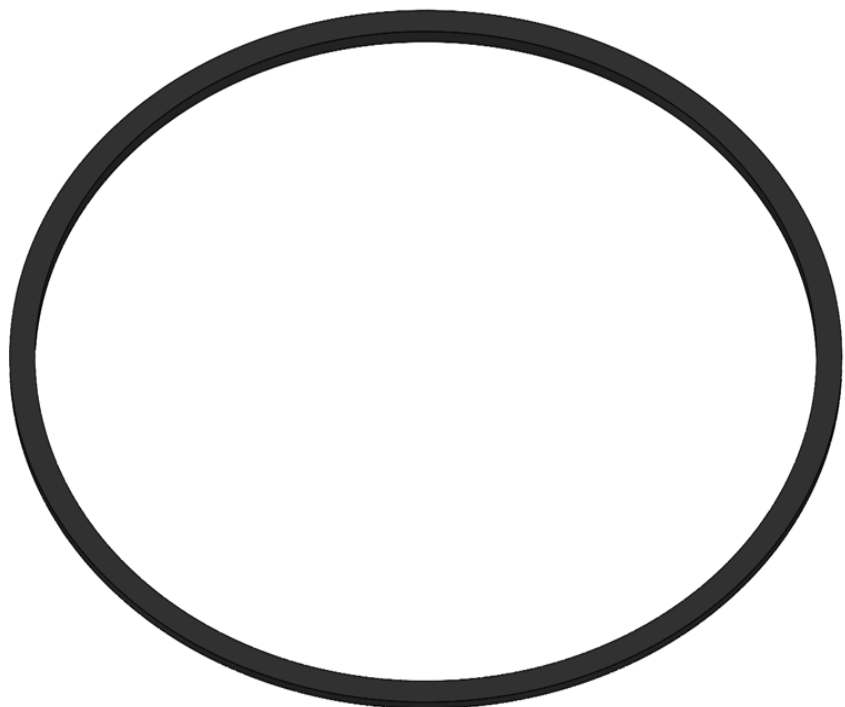


Figure 35 : Lab Sealing Model

4.7 Spinner

The spinner, also known as the nose cone, is the aerodynamic enclosure located at the very front of the wind turbine rotor hub. Although it may appear to be a simple cover, the spinner performs several essential mechanical, environmental, aerodynamic, and safety functions that directly influence turbine reliability and performance. It is typically made from lightweight composite materials to maintain strength while minimizing rotational inertia added to the rotor assembly.

Aerodynamic function

One of the primary purposes of the spinner is to streamline airflow around the hub region, which otherwise represents a large aerodynamic obstruction. The smooth, tapered geometry of the spinner guides incoming wind around the rotating blades and hub, reducing turbulence and aerodynamic drag. This aerodynamic smoothing increases turbine efficiency by maximizing the usable wind energy captured by the blades. Without a spinner, unwanted air separation and eddies at the hub would lower the turbine's power performance and create noisy, unstable airflow.

4.7.1 CAD Model of Spinner

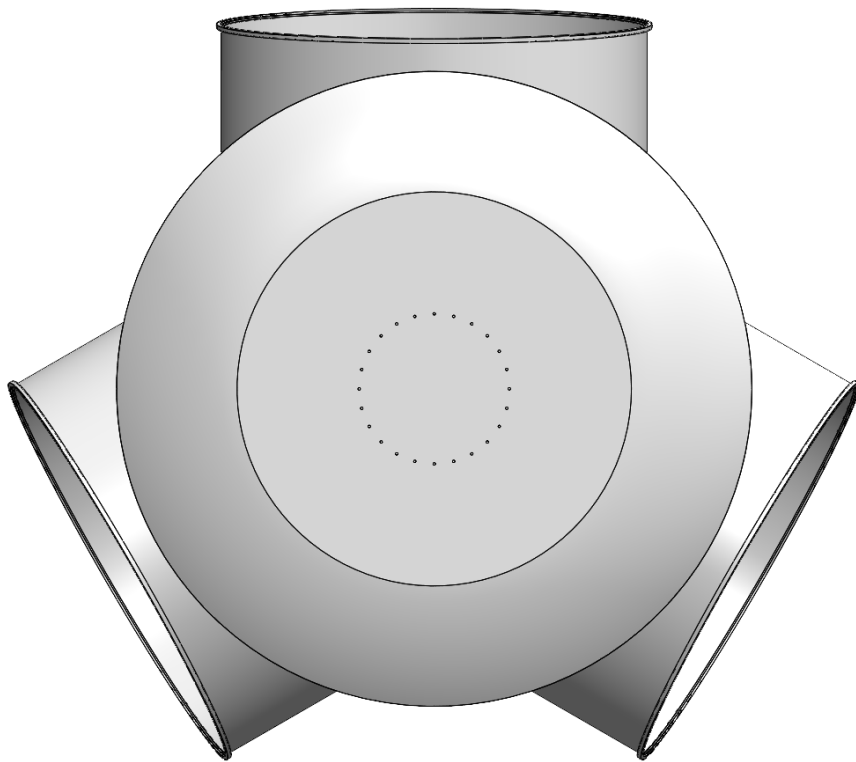


Figure 36 : Spinner CAD Model of Optimus Syria

Protection of Internal components

Internally, the spinner protects the critical mechanisms housed inside the hub, including pitch bearings, hydraulic or electric pitch actuators, lubrication lines, cabling, control electronics, and blade-root fastenings. It serves as a barrier against environmental contaminants such as rain, UV light, snow, sand, insects, and dust. This function is particularly important in harsh operating environments, such as Syria, where desert dust, high summer temperatures, and seasonal precipitation could cause serious wear, corrosion, and premature degradation of mechanical and lubricated components. The controlled environment created by the spinner helps extend the service life of bearings, reduces grease contamination, minimizes corrosion, and supports stable operating temperatures inside the hub.

Safety and Maintainability

Beyond mechanical protection, the spinner provides a safe, enclosed workspace for technicians during on-hub maintenance and inspection activities. Turbine hubs are not exposed to the external environment because the spinner acts like a protective dome, allowing maintenance staff to enter the hub interior and work comfortably without direct exposure to rain, wind, or extreme sunlight. This is especially useful for emergency shutdown repairs or winter servicing, where performing tasks inside a protected enclosure significantly enhances safety and reduces downtime.

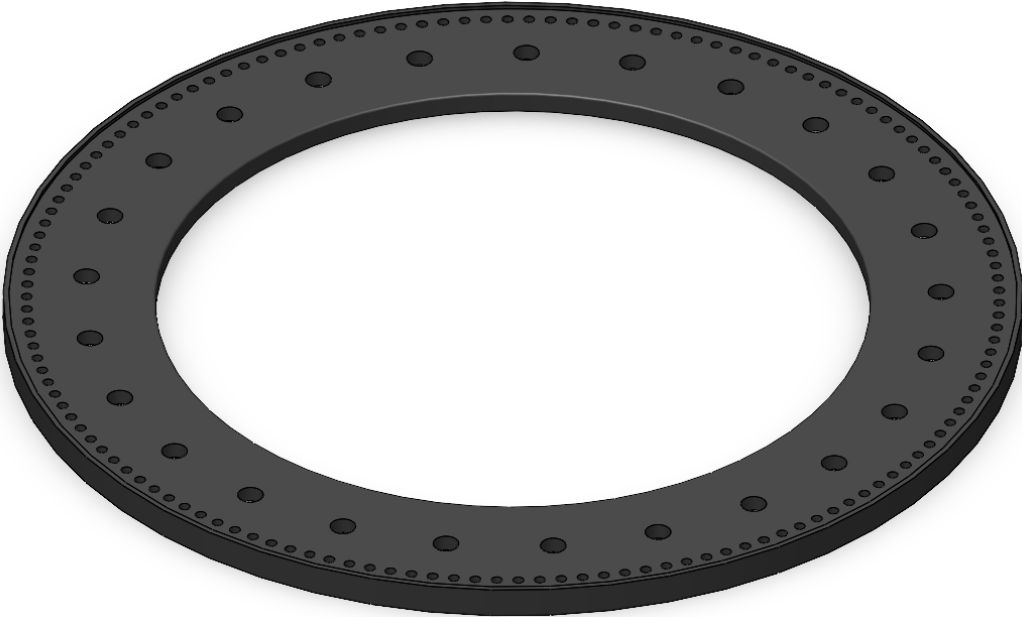
4.8 Stiffening Ring

An additional stiffening ring is incorporated at the blade–hub interface to enhance the local structural stiffness and improve the transfer of loads from the blade into the hub. This region is subjected to high bending moments, cyclic loads, and stress concentrations around the blade bearing seat and bolt connections. The stiffening ring increases the local section stiffness and helps distribute forces and moments more uniformly, thereby reducing peak stresses and limiting local deformation. By improving the stiffness of the blade bearing support, the ring also ensures a more even load distribution within the bearing, which contributes to improved bearing performance and fatigue life. Furthermore, the use of a localized stiffening ring allows targeted reinforcement without significantly increasing the overall hub mass, resulting in a structurally efficient and cost-effective design solution.

Stiffening Ring	
Total Weight	3.5 T
Material	EN-GJS-400-18
Number of Rings	3 (Each per blade)
Holes for Bolts on Inner BCD	25 × D90
Holes for Bolts on outer BCD	142 × D38
Ring Thickness	100 mm

Table 16 : Specification of Stiffening Ring

4.8.1 CAD Model of Stiffening Ring

*Figure 37 : Stiffening Ring CAD Model of Optimus Syria*

4.9 Complete Assembly of Rotor Hub and Pitch System

The complete assembly integrates all major components of the rotor hub and pitch system into a single functional unit, including the rotor hub, blade bearings, pitch actuation components, lubrication elements, and stiffening rings. The arrangement ensures effective load transfer from the blades to the main shaft while enabling reliable and accurate blade pitch control. The assembly model also confirms the compatibility of individual components and demonstrates the feasibility of the proposed design for the Optimus Syria wind turbine.

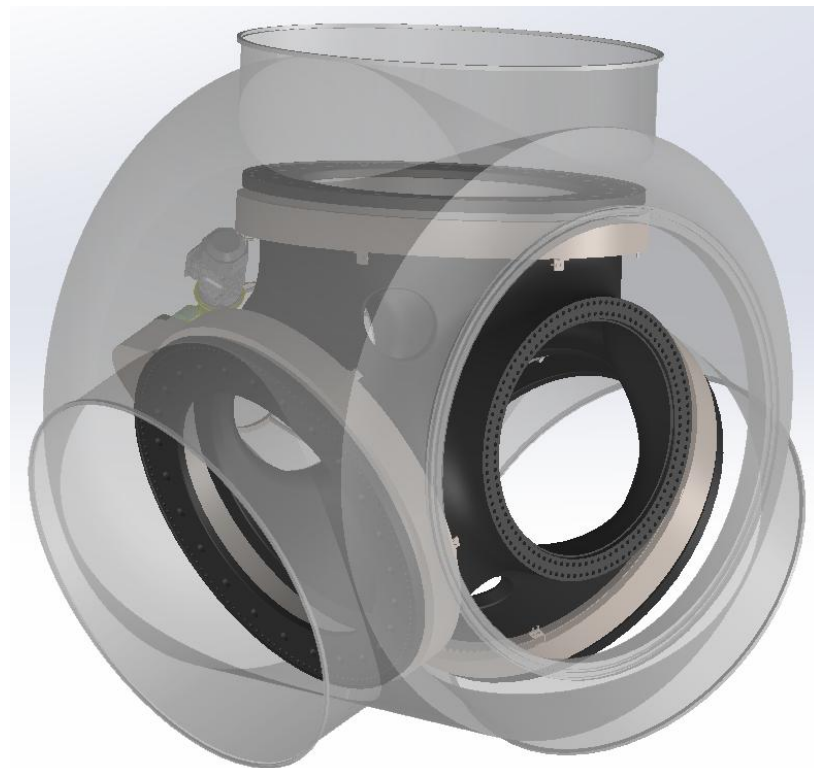


Figure 38 : Shaft side view of the complete rotor hub and pitch system assembly of Optimus Syria



Figure 39 : Complete rotor hub and pitch system assembly of Optimus Syria

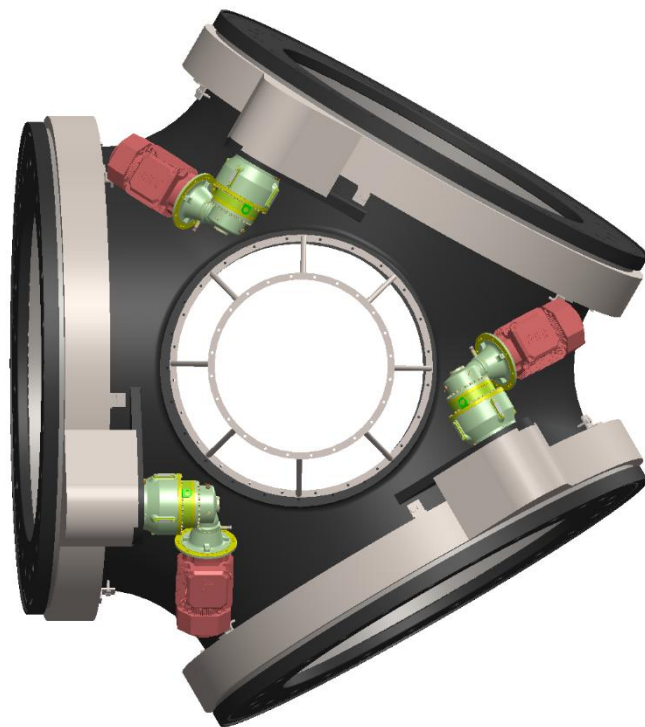


Figure 40 : Assembly without spinner

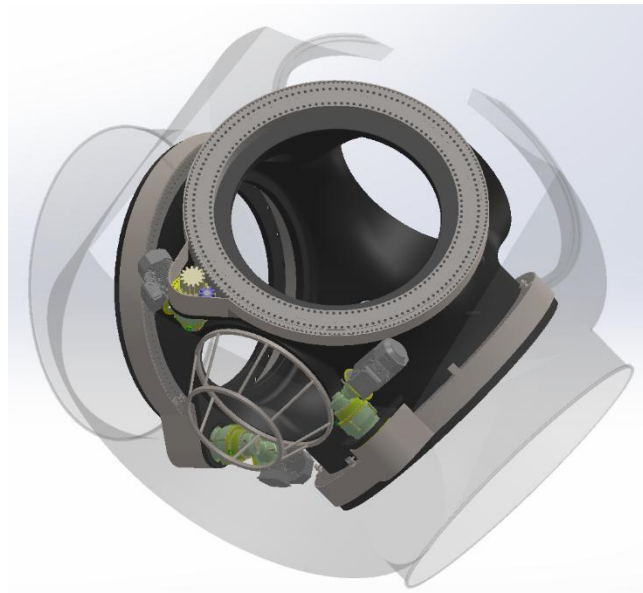


Figure 41 : Top Cross-section view Assembly

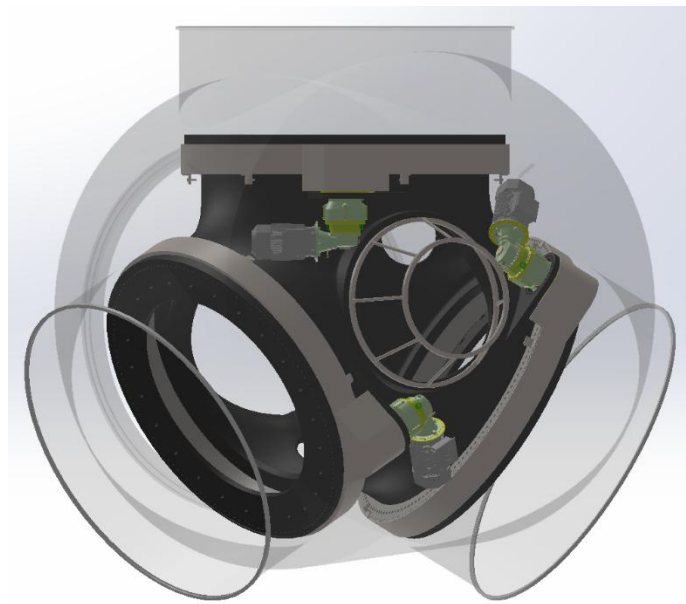


Figure 42: View from front side

4.10 Part List

Component	Quantity
Rotor Hub	1
Additional Stiffening Ring	3
Pitch Motor	3
Pitch Gearbox	3
Pitch Bearing	3
Pitch Bearing Cover	3
Lubrication pinion	3
Spinner	1
Spinner connection ring	1
Blade Labyrinth Seal	3
Nacelle Labyrinth Seal	1
Battery	1
Inverter	1

Table 17 : Part List

5. External Supporters

The team received a lot of assistance from outside supporters. A basic phase in the design process to acquire information and even estimated alternatives for the various components was contacting the various manufacturers for the various components to gain vital input on the progress. The team would like to thank all the manufacturers and suppliers for their time and tremendous assistance with this student project.

Guido Claßen

Customer Application Engineering

Mobility & Wind Industries

Bonfiglioli Deutschland GmbH

G.Classen@bonfiglioli.de

+49 21312988221

Moritz Abrath

ABB Deutschland

Moritz.abrath@de.abb.com

6. Maintenance & Strategies

Proper upkeep of the rotor hub and pitch system is essential to keep a wind turbine operating safely, efficiently, and reliably. These components are central to power production and turbine control, and any failure can lead to reduced output, unexpected shutdowns, or serious structural damage. The following section presents a maintenance overview organized by individual components.[34]

Pitch Bearing

The maintenance of the pitch bearing is carried out through periodic inspections to ensure reliable operation, adequate lubrication, and structural integrity.

Semi-annual maintenance activities primarily focus on condition monitoring and early detection of wear. These include visual inspection of the pitch bearing, verification of gear wear through measurement, inspection of the lubrication system, and relubrication of the gear ring and drive gear where required. In addition, the condition of the grease supply system is checked to ensure proper distribution.

Annual maintenance activities include all semi-annual tasks, with added emphasis on mechanical integrity. This involves torque verification of the bearing-to-hub bolted connections and a detailed inspection of the bearing housing to confirm structural stability and alignment.

Pitch System

The pitch system maintenance strategy is designed to ensure precise blade positioning, reliable actuation, and safe operation under all conditions.

Semi-annual inspections include verification of the blade zero-degree reference position, inspection of battery voltage levels, sensor functionality checks, and visual inspection of critical fastening elements such as pitch motor fixing bolts and control cabinet support bolts.

Annual maintenance activities extend these checks by incorporating torque verification of gearbox-to-hub connections, inspection of gearbox oil level, and confirmation of correct pitch motor alignment. Electrical components, including sensors and backup power units, are also examined in detail to ensure continued operational reliability.

Long-term maintenance actions, performed at extended intervals (approximately every five years), include pitch gearbox oil replacement and lubrication of gearbox bearings, in line with manufacturer recommendations.

Hub and Spinner

The hub and spinner are maintained through scheduled inspections aimed at preserving structural integrity, operational safety, and accessibility for service personnel.

Semi-annual maintenance activities include a general inspection of the spinner surface to detect cracks, damage, or signs of material degradation. The spinner mounting brackets and their connecting bolts are visually inspected to ensure proper fastening. In addition, the hub interior and exterior surfaces are cleaned to remove accumulated dust, grease residues, and contaminants that may affect inspection quality or component lifetime.

Annual maintenance activities build upon the semi-annual inspections and place particular emphasis on mechanical connections. This includes torque verification of the hub-to-shaft bolted joint as well as the bolts associated with internal access components, such as foot pedals or service supports. These checks ensure that all load-bearing connections remain secure under operational and dynamic loading conditions.[34]

7. Weight and cost

Item	Qty	Weight	Cost per unit	Total Cost
Hub	1	35 T	70,000 €	70,000 €
Additional stiffening ring	3	2.7 T	5400 €	16,200 €
Pitch Drive	3	800 Kg	6333 €	19,000 €
Battery	1	43.6 Kg	1980 €	1980 €
Inverter	1	29 Kg	1900 €	1900 €
Blade Bearing	3	6.6 T	33,000 €	99,000 €
Blade Bearing cover	3	1 T	2000 €	6,000 €
Spinner	1	1.3 T	4000 €	4,000 €
Fastening components and Cable				10,000 €
Total				2.28,000 €

Table 18 : Weight and Cost of all the Components

8. Environmental Life Cycle Assessment

Wind energy plays a crucial role in the transition toward low-carbon and sustainable power generation systems. As a renewable energy source, wind turbines generate electricity without direct greenhouse gas emissions during operation. However, the overall environmental footprint of wind turbines cannot be neglected, as significant emissions arise during the manufacturing, transportation, and end-of-life stages of their components. These lifecycle-related emissions are primarily associated with energy-intensive production processes and the extraction and processing of raw materials.

Although wind turbines exhibit high environmental performance during their operational phase, several studies indicate that the majority of lifecycle emissions are concentrated in the production and installation stages. The conversion of raw materials into structural and mechanical components, particularly for large wind turbine assemblies, requires substantial energy input. Consequently, evaluating environmental impacts over the entire lifecycle is essential for a realistic assessment of sustainability.

Life Cycle Assessment (LCA) has been widely applied to quantify the environmental impacts of wind energy systems. Previous research, such as the work conducted by Haapala, demonstrated that key turbine components—including the rotor assembly, nacelle, and tower—are major contributors to overall CO₂ emissions due to their material composition and manufacturing intensity. In addition, transportation logistics and end-of-life treatment play an important role in determining the total environmental impact. High recycling rates for metallic materials can significantly reduce lifecycle emissions, while non-recyclable materials contribute negatively to the overall environmental balance.

Building upon established LCA methodologies, this chapter evaluates the environmental impact of selected rotor hub and pitch system components of the Optimus Syria wind turbine. The assessment focuses on material production emissions, transportation-related emissions, and end-of-life considerations to provide a simplified yet representative estimation of CO₂ emissions associated with the proposed design.[35]

Material Emission calculation

The first step in the environmental assessment involves estimating material-related carbon dioxide emissions for the main components of the rotor hub and pitch system. Each material used in the design is characterized by a specific emission factor, expressed in kilograms of CO₂ per kilogram of material (kg CO₂/kg). These factors account for emissions generated during raw material extraction and manufacturing processes.

The Optimus Syria design primarily utilizes EN-GJS-400-18 cast iron, alloy steel (42CrMo4), and glass fiber-reinforced materials. Among these, EN-GJS-400-18 contributes significantly to the total emissions due to its extensive use in heavy structural components such as the rotor hub. The material-related

emissions are calculated by multiplying the mass of each component by its corresponding emission factor, resulting in the total manufacturing emissions per component.

Transportation Emissions

In addition to manufacturing emissions, transportation of turbine components contributes to the overall carbon footprint. For the Optimus Syria project, long-distance transportation is assumed, reflecting realistic global supply chains for wind turbine components. The transportation scenario considers sea freight followed by road transport to the installation site.

Emissions are calculated based on transported mass and distance, using standard emission factors for maritime and road transport. A load factor is included to account for partial loading and return trips, ensuring a conservative estimation of transportation-related CO₂ emissions.

End Of Life Impact

The final lifecycle stage involves the recycling or disposal of turbine materials. Metallic materials such as steel, cast iron, and aluminium exhibit high recyclability, with recycling rates assumed to reach up to 90%. Recycling significantly offsets emissions by reducing the need for primary material production. In contrast, composite materials such as glass fibre are typically not recyclable and are assumed to be disposed of in landfills, contributing negatively to the environmental profile.

Proper end-of-life management plays a vital role in minimizing lifecycle emissions and improving the overall sustainability of wind turbine systems. The assumptions made in this assessment reflect commonly applied practices in wind turbine lifecycle studies.

Result

The total CO₂ emissions for each component, combining material, transportation, and end-of-life impacts, are summarized in the table below:

Component	Material Emissions (kg CO ₂)	Transportation	Total Emissions
		Emissions (kg CO ₂)	(kg CO ₂)
Rotor Hub (35 T, cast iron)	24,500	4000	28,500
Blade Bearings (3 × 6.6 T)	13,860	2100	15,960
Additional Stiffening Rings (3 × 2.7 T)	5670	900	6570
Pitch Drives (3 × 800 Kg)	3600	600	4200
Spinner (1.3 T)	2600	520	3120
Lubrication (Oil & Grease)	375	60	435

Table 19 : Co2 Emission from the Components lifecycle

9. Project Planning and Task Allocation

The development of the rotor hub and pitch system for the 5 MW onshore wind turbine Optimus Syria was carried out through close collaboration within a four-member project team. To manage the scope of the work efficiently, the overall design activities were organized into clearly defined tasks and allocated according to the technical competencies of each team member. Continuous coordination was maintained throughout the project through regular team discussions, complemented by weekly review meetings with the project supervisor and project manager. These interactions ensured timely feedback, facilitated technical decision-making, and supported steady project progress.

Working on a large-scale wind turbine system provided an important opportunity to bridge theoretical engineering principles with practical design implementation. The integration of the rotor hub and pitch system demanded repeated design refinements and careful validation across subsystems, which increased the complexity and duration of the work. Occasional limitations in accessing specialized technical references further added to the challenge.

Despite these constraints, the team adapted effectively by prioritizing tasks, exploring alternative information sources, and maintaining a disciplined workflow.

The final outcome of the project is a mechanically robust rotor hub capable of accommodating operational loads, together with a pitch system designed to support both aerodynamic control and load reduction. In addition to the technical achievements, the project reinforced the value of teamwork and structured collaboration in addressing complex engineering problems. The allocation of responsibilities among the team members is presented in the following table.

Section	Task Name	Report Writer	Contributors (Design and Contributions)
	Introduction	Muthu, Adharsh	-
	Relevant Standards and Guidelines	Muthu, Adharsh, Sikandar	-
	Loads	Muthu, Adharsh, Sikandar	Dhruvin
4.1	Rotor Hub	Dhruvin, Muthu, Adharsh	Dhruvin
4.1.1	Shapes of the Hub	Muthu, Adharsh	Dhruvin, Muthu
4.1.2	Material of the Hub	Dhruvin, Muthu, Adharsh	Dhruvin
4.1.3	CAD Design & Dimensions	Dhruvin	Dhruvin

4.2.1	Classification of Pitch System	Muthu, Adharsh	Dhruvin, Muthu, Adharsh
4.2.1	Calculation of Pitch System	Muthu	Muthu
4.2.2	Comparison between different concepts of Pitch System	Muthu, Adharsh, Sikandar	Dhruvin, Muthu, Adharsh
4.2.3.2	Pitch Drive Selection	Muthu, Adharsh	Dhruvin, Muthu, Adharsh
4.2.3.4	CAD Model of Motor	Dhruvin, Muthu	Adharsh, Muthu, Sikandar
4.2.3.5	CAD Model of Gearbox	Adharsh	Adharsh, Sikandar
4.2.3.7	CAD Model of Pitch Drive Assembly	Dhruvin, Adharsh	Dhruvin, Adharsh, Sikandar
4.2.3.8	Backup Supply System	Muthu, Adharsh	Muthu
4.4.1	Type of Bearings	Muthu, Adharsh	Adharsh, Sikandar
4.4.2.1	Comparison of Inner Ring and Outer Ring Configurations	Muthu, Adharsh	Adharsh, Sikandar
4.4.3	Dimensioning of Three Row Roller bearing	Muthu, Adharsh	Dhruvin, Adharsh, Sikandar
4.4.4	Pitch bearing Safety Factor Calculation	Muthu, Adharsh	Adharsh, Sikandar
4.4.5	CAD Model of Bearing and its Dimensions	Dhruvin	Adharsh, Sikandar
4.5	Lubrication system	Muthu, Adharsh, Sikandar	Muthu
4.5.3	Grease Volume Calculation	Muthu, Adharsh	Muthu, Sikandar
4.5.5	Lubrication Pump & Reservoir Calculation	Muthu, Adharsh	Muthu

4.5.7	CAD Model of Lubrication Pinion	Dhruvin, Muthu	Dhruvin, Sikandar
4.6	Labyrinth Sealing	Dhruvin	Dhruvin
4.7.1	CAD Model of Spinner	Dhruvin	Dhruvin
4.8	Stiffening Ring	Muthu	Dhruvin
4.8.1	CAD Model of Stiffening Ring	Dhruvin	Dhruvin
4.9	Complete Assembly of Rotor Hub and Pitch System	Dhruvin	Dhruvin
5	Maintenance Strategies	Muthu, Adharsh	Muthu
6	Weight and Cost	Dhruvin	Dhruvin
7	Environmental Life Cycle Assessment	Muthu, Adharsh	Muthu, Adharsh
9	Key Takeaways from the Project	Muthu, Adharsh, Sikandar	Sikandar
10	Project Summary and Future Work	Muthu, Adharsh, Sikandar	Sikandar
	Annextures	Dhruvin	Dhruvin
	Final Report correction and check	Dhruvin	Dhruvin

10. Key Takeaways from the Project

The Optimus Syria project, which focused on the design of the rotor hub and pitch system for a 5 MW onshore wind turbine, provided valuable technical and professional learning experiences. Throughout the project, the team developed a deeper understanding of how complex mechanical systems are designed, analysed, and integrated within a large-scale wind energy application.

Adhering to regular milestones and presentation schedules highlighted the importance of structured planning and effective time management. Managing weekly deliverables required consistent effort and prioritization, which improved our ability to work under defined deadlines. Repeated technical presentations also strengthened our confidence in communicating engineering concepts clearly and responding constructively to technical feedback.

Close collaboration within the team, as well as continuous interaction with the project supervisor, significantly enhanced our communication and coordination skills. These interactions emphasized the value of teamwork, constructive discussion, and shared responsibility when addressing technical challenges. The project also contributed to a strong technical foundation in hub and pitch system design, including an improved understanding of component functionality, material selection, and structural behaviour under operational loads.

In addition, extensive use of engineering software tools such as SolidWorks for mechanical modelling and MATLAB for analytical evaluations improved our practical skills and familiarity with industry-relevant design workflows. Overall, the project reinforced the importance of systematic problem-solving, adaptability, and collaboration in successfully completing complex engineering tasks.

11. Project Summary and Future Work

The Optimus Syria project focused on the conceptual and preliminary design of the rotor hub and pitch system for a 5 MW onshore wind turbine, with particular emphasis on structural integrity, operational reliability, and suitability for challenging operating conditions. Throughout the project, internationally recognized standards such as DNV, IEC, and ISO were applied to ensure that the proposed design meets accepted safety and performance requirements for modern wind turbines.

A comprehensive load definition was established based on simulation data and reference values from comparable turbine systems. These loads formed the basis for the structural dimensioning of the rotor hub, blade bearing, and pitch system components. The star-shaped cast hub design, manufactured from spheroidal graphite cast iron (EN-GJS-400-18), was selected due to its favourable balance between strength, manufacturability, weight, and maintenance accessibility. The integration of an additional stiffening ring further enhanced local stiffness at the blade–hub interface, contributing to improved load distribution and reduced stress concentrations.

For blade pitch actuation, an electric pitch system was selected as the most suitable solution for the Optimus Syria turbine. Detailed calculations were performed to determine the required pitch torque, bearing friction effects, gear ratios, and motor-side torque demands. Based on these results, a synchronous AC reluctance motor combined with a multi-stage A planetary gearbox was chosen to meet the required performance, efficiency, and reliability criteria. The pitch bearing was designed as a three-row roller bearing to accommodate the high bending moments and combined axial and radial loads, ensuring sufficient safety margins against Hertzian contact stress and gear tooth failure.

Special attention was given to turbine safety and operability through the design of a robust backup power supply system. A lithium iron phosphate (LiFePO₄) battery system was selected to guarantee reliable emergency pitch operation under grid failure scenarios, which is particularly critical given the anticipated grid instability and harsh environmental conditions in Syria.

Overall, the developed rotor hub and pitch system concept for Optimus Syria demonstrates a technically sound and balanced design that integrates structural robustness, reliable control, and practical manufacturability. As future work, the design could be further refined through detailed finite element analysis, fatigue life assessment, and validation against full design load case (DLC) envelopes. Additionally, further optimization of component mass and investigation of advanced manufacturing techniques could contribute to improved performance and cost efficiency in subsequent development stages.

References

- [1] United Nations Development Programme, “Energy and Environment Programme – Syria,” UNDP, 2020. [Online]. Available: <https://www.undp.org/syria>
- [2] DNV-ST-0361, Machinery for wind turbines, DNV GL, September, 2016.
- [3] GL, „Guidelines for certification of the wind turbines, “ GL, 2010.
- [4] G. Erich Hau Dipl.–Ing Munich, Wind Turbines Fundamentals, Technologies, Application, Economics, Munich, 2012.
- [5] A. Cooperman, „Large Castings for Wind Turbines, “ National Renewable Energy Laboratory (NREL), 2023. [Online]. Available: <https://www.nrel.gov/docs/fy23osti/86352.pdf>.
- [6] C. Hollas et al., „Hollow Forged AHD Steel Rotor Shafts for Wind Turbines: A Case Study on Power Density, Costs and GWP, “Wind Energy Science, 2026. [Online].
- [7] R. Gasch and J. Twele, Wind Power Plants: Fundamentals, Design, Construction and Operation, Springer, Berlin/Heidelberg, 2012.
- [8] P.-i. H. W. Proff. Peter Quell, „Rotor Hub and flanges, “in *Machinery Components*, 2024.
- [9] I. D. SARAC V., „Synchronous Motor of Permanent Magnet compared to Asynchronous Induction Moto”, “Electrotechnical Electronica, Automatic (EEA), e. %1 von %2, vol. 65, Nr. ISSN 1582-5175, pp. no. 4, pp. 51-58, 2017.
- [10] U. o. Tennessee. [Online]. Available:
https://web.eecs.utk.edu/~kaisun/Backup/ECE325_Fall2016/ECE325_6-InductionMotors_4.pdf.
- [11] &. A. P. &. A.-A. I. &. A. Enesiasizehiyahaya, Analysis of Power flow and Torque of Asynchronous Induction Motor Equivalent circuits. 3., “2013.
- [12] B. M. S. B. I. M. A.Y. Achour, „Passivity-based current controller design for a permanent-magnet synchronous motor, ISA Transactions, Bd. Volume 48, Nr. Issue 3,2009,
<https://doi.org/10.1016/j.isatra.2009.04.004>
- [13] M. Ç. Yıldırım ÖZÜPAK, „DESIGN OF THE PERMANENT MAGNET SYNCHRONOUS MOTOR USED IN ELECTRIC VEHICLES WITH THE HELP OF THE PARTICLE SWARM ALGORITHM AND ANSYS-MAXWELL, “ 21 01 2025. [Online]. Available:
<https://dergipark.org.tr/en/download/article-file/3212091>
- [14] H. R. A. K. A. V. T. A. E. B. A. &. L. D. V.] Heidari, A Review of Synchronous Reluctance Motor-Drive Advancements. Sustainability, 13(2), 729, “ Bd. 13(2), Nr.
<https://doi.org/10.3390/su13020729>, 2021
- [15] M. C. Vladan Vujičić, „Characteristics of Switched Reluctance Generator operating with Derishzadeh converter, “ in *IcETRAN*, Zlatibor, Serbia, 2016.

- [16] “Direct Current Motors.” CEDS Duradrive, CEDS Duradrive, [Online]. Available: www.ceds-duradrive.de/en/technologien/direct-current-motors/.
- [17] K. B. P. F. Jan Wenske, Wind Turbine System Design. Volume 1: Nacelles, drivetrains and verification, IET - The Institution of Engineering and Technology, December 2022.
- [18] L.-C. A. (n.d.). „Slewing bearings: “Product catalogue. Liebherr, [Online]. Available: https://www-assets.liebherr.com/media/bu-media/lhbucot/documents/cot_grosswaelzlager/sticky_notes/liebherr-slewing-bearings-product-catalogue-en-metric-web.pdf.
- [19] ABB, “Power and Productivity for a Better World,” ABB. [Online]. Available: <https://new.abb.com/your-page-here>.
- [20] Kurt.Energy, „Eric Verhulst 2024 Wind turbine pitch control and emergency shutdown, “<https://kurt.energy/wind-turbine-pitch-control-and-emergency-shutdown/>, (accessed 28 Dec 2024).
- [21] J. W. J. Q. a. Q. H. Bixiao G, „The Lithium-ion Battery Standby Power of Wind Turbine Pitch System Energy Procedia, “ p. 105 3539–44, 2017.
- [22] LIONTRON GmbH, LiFePO₄ Battery LX48-100 Datasheet, LIONTRON, Germany. [Online]. Available: https://liontron.com/download/english/LIONTRON-Datasheet_LX48-100_EN-1.pdf
- [23] Victron Energy B.V., MultiPlus-II 120 V Inverter/Charger Datasheet, Victron Energy, Almere, The Netherlands. [Online]. Available: <https://www.victronenergy.com/upload/documents/Datasheet-MultiPlus-II-120V-EN-.pdf>
- [24] K. a. B. A. & B. E. & G. Behnke, Pitch systems concepts Ans Design, 2022.
- [25] thyssenkrupp-rotheerde, “thyssenkrupp-rotheerde, 08 11 2024. [Online]. Available: <https://www.thyssenkrupp-rotheerde.com/en/industries/renewable-energy/wind-energy/pitch-bearing>. [Zugriff am 03 01 2025].
- [26] IMO, “IMO-Slew drives and Slewing ring, 2016. [Online]. Available: https://www.youtube.com/watch?v=eVXnD0_L0c4. [Zugriff am 03 01 2025].
- [27] M. O. M. Y. G. a. J. K. Stammler, „Wind Turbine Design Guideline DG03: Yaw and Pitch Bearings, “National Renewable Energy Laboratory (NREL), Bd. 2, 2024.
- [28] Senvion Products, “2024. [Online]. Available: <https://www.senvion.in/products/4-2m160/>. [Zugriff am 03 01 2025].
- [29] D. e. a. Muhs, Roloff/Matek Maschinen elemente, Normung Berechnung Gestaltung, Auflage; Wiesbaden Friedr. Vieweg & Sohn Verlag/GWV Fachverlag GmbH, 2005.
- [30] ABB, “Lubrication systems for wind turbines,” ABB Group. [Online]. Available: <https://new.abb.com/service/motion/wind/lubrication>.

- [31] SKF, “SKF LGWM 2 – High load, wide temperature range grease,” SKF Group. [Online]. Available: <https://www.skf.com/group/products/lubricationmanagement/lubricants/greases/skf-lgwm-2>
- [32] SKF, “KFG lubrication pump for centralized lubrication systems,” SKF Group. [Online]. Available: <https://www.skf.com/group/products/lubrication-management/lubrication-systems/kfg-system>.
- [33] SKF, “SKF-LP02-Lubrication pinion, 2024. [Online]. Available: https://cdn.skfmediahub.skf.com/api/public/0901d196806c2ca9/pdf_preview_medium/0901d196806c2ca9_pdf_preview_medium.pdf.
- [34] Envision, „Envision Wind Power, “ 2025. [Online]. Available: <https://www.envision-group.com/en/windturbines.html>.
- [35] ISO, “ISO 14040: Environmental management—Life cycle assessment—Principles and framework,” International Organization for Standardization, Geneva, Switzerland, 2006.
- [36] Mr. Christian Bulligk, Three Rows roller bearing Dimensioning of the Raceway system & Loads, Flensburg, 2024.

Annextures

A-Loads

B- Project Order

C- Rotor Hub Optimus Syria

D- Pitch Bearing

E- Spinner of Optimus Syria

F-Assembly of rotor hub and pitch system of Optimus Syria

Maximum Loads Simulation	Fx	Fy	Fz	Resultant Force (Fxy)	Edgewise Bending (Mx)	Flapwise Bending (My)	Pitching Torque (Mz)	Resultant Bending (Mxy)
-	kN	kN	kN	kNm	kNm	kNm	kNm	KNm
-	1153	1267	3252	1327	4243	3517	1594	4674
Blade Root Forces and Bending Moments For Optimus Syria								
Design Loads(Supervisor)	Fx	Fy	Fz	Resultant Force (Fxy)	Edgewise Bending (Mx)	Flapwise Bending (My)	Pitching Torque (Mz)	Resultant Bending (Mxy)
-	kN	kN	kN	kNm	kNm	kNm	kNm	KNm
-	840	630	650	730	17000	36000	370	30000

TEAM PROJECT ORDER CONTRACT

Project Name: Optimus Syria

Sub-Team: Rotor Hub and Pitch System Client: Bakhtyar Karim (Head of Project)

Date: 13.07.2025

Project Number: 01.2025

Team Leader: Dhruvin Bhupatbhai Kakdiya

Problem Description

1. The Rotor Hub and Pitch System sub-team is responsible for designing the mechanical interface between the rotor blades and the nacelle, as well as the pitch actuation mechanism.
2. This includes choosing a hub concept, sizing pitch bearings, and selecting the pitch actuation method (hydraulic or electric). Close coordination with the Rotor Blade, Loads, and Control teams is necessary for successful integration.

Goals

- Select an appropriate hub type and pitch mechanism
- Design blade-to-hub connection considering loads and geometry
- Decide on electric or hydraulic pitch actuation and justify choice
- Consider redundancy, safety, and pitch range in design
- Ensure compatibility with aerodynamic and control needs

Deliverables

- Hub type and layout selection
- Pitch mechanism concept and actuator sizing
- Blade mounting sketches or schematics
- Analysis of mechanical constraints and operational limits
- Contributions to the final report and final presentation

Milestones & Deadlines

Milestone: Initial preparations Deadline: 24th Aug – 7th Sep 2025

Comments: Study pitch systems, actuator types, and hub options

Milestone: Concept freeze Deadline: 13th Sep 2025

Comments: Select hub type and actuation method

Milestone: Load principle measurements Deadline: 7th Oct 2025

Comments: Use loads from Aero & Structure teams to size components

Milestone: Interface freeze Deadline: 28th Oct 2025

Comments: Confirm blade interface and actuator layout

Milestone: Input freeze for simulation Deadline: 18th Nov 2025

Comments: Provide key parameters for pitch control modeling

Milestone: Design freeze Deadline: 9th Dec 2025

Comments: Final hub and pitch system design locked

Milestone: Final Report Deadline: Week 5/2026 (27 Jan 2026)

Comments: Submit mechanical pitch and hub documentation

Milestone: Final Presentation Deadline: Week 5/2026 (25–31 Jan 2026)

Comments: Present system concept, justification, and performance

Team Leader Duties

- Organize team efforts and assign component design tasks
- Communicate frequently with Aero, Structure, and Control teams
- Supervise sizing and comparison of pitch actuation systems
- Maintain detailed records of component specs and design logic

- Inform the Head of Project about challenges and updates
- Ensure delivery of final design documentation and sketches

Restrictions

[To be completed by the team leader: List any specific technical, academic, or organizational restrictions that apply to your team.]

Risk Management

Risk: Improper sizing of pitch actuator

Action: Use safety margins and refer to load assumptions

Risk: Conflict between control requirements and mechanical limits

Action: Define acceptable pitch angles and rates early

Risk: Mechanical integration issues with blade or nacelle

Action: Coordinate dimensions and interfaces with other sub-teams

Signatures

Role: Head of Project

Name: Bakhtyar Karim

Signature: 

Role: Sub-Team Leader

Name: Dhruvin Bhupatbhai Kakdiya

Signature: 

